Science of the Total Environment 1003 (2025) 180640

Contents lists available at ScienceDirect

Science of the Total Environment

journal homepage: www.elsevier.com/locate/scitotenv

Hydrogeochemical characterization and human health risk assessment for heavy metal contamination in coastal aquifers: A case study in Satkhira District, Bangladesh

Md Yeasir Hasan [a,h], Xiaolang Zhang [b], Chao Xu [a,*], Jay Sui Tung [a], Abir Ahmed Rifat [c], M. Shahriar Sonet [d], Abdulla-Al Kafy [e], Shaikh Sadiqur Rahman [f], Md Jamal Faruque [g,h]

[a] Department of Geosciences, Texas Tech University, Lubbock, TX 79409, USA
[b] Department of Geosciences, Florida Atlantic University, Boca Raton, FL 33431, USA
[c] Department of Mathematics, University of Chittagong, Chittagong 4331, Bangladesh
[d] Geospatial Information Sciences, University of Texas at Dallas, 800 W Campbell Rd, Richardson, TX 75080, USA
[e] Department of Geography & the Environment, University of Texas at Austin, Austin, TX 78712, USA
[f] Nebraska Cooperative Fish and Wildlife Research Unit, University of Nebraska-Lincoln, Lincoln, NE 68583, USA
[g] Water Resources and Environmental Management, University of Twente, Drienerlolaan 5, 7522 NB Enschede, Netherlands
[h] Lab of Bangladesh Agricultural Development Corporation (BADC), Jashore, Bangladesh

HIGHLIGHTS

- Identified synergistic effect of salinization and heavy metals in coastal areas
- This coastal aquifer contains higher carcinogenic and non-carcinogenic risks.
- The study area demonstrates greater amount of salinity intrusion.
- Assessed health risks associated with saltwater-prone groundwater routes
- CCD and RSM were used for the distribution of statistical approaches.

GRAPHICAL ABSTRACT

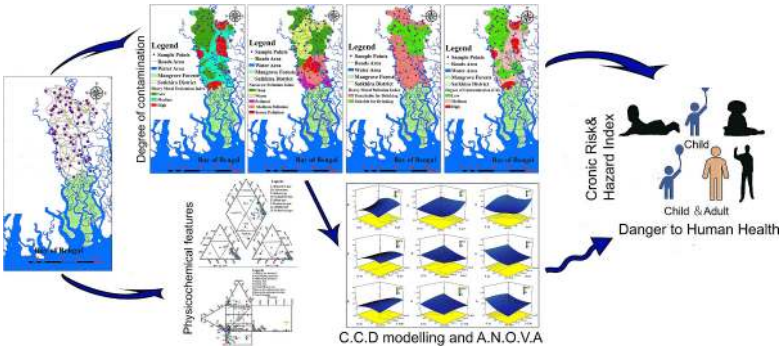

ARTICLE INFO

Keywords:
Environmental geochemistry
Heavy metal contamination
Source apportionment
Health risk assessment
Coastal aquifer vulnerability
Environmental toxicology

ABSTRACT

This study investigates the health risks associated with polluted groundwater in the coastal region of Satkhira District, Bangladesh, where high population density exacerbates exposure to contaminants. Analyzing 66 groundwater samples collected from January to June 2023, we explored the spatial distribution patterns and hydrochemical composition, with a particular focus on heavy metals. Utilizing Response Surface Methodology, we optimized the synthesis ratios of heavy metals and assessed their correlations with various indicators through variance analysis. Additionally, Pearson's correlation and Principal Component Analysis were applied to identify pollution sources and groundwater characteristics. The results, illustrated through Piper and Drove diagrams, indicated that the majority of samples were classified as sodium-chloride (Na—Cl) facies, highlighting a significant risk of saltwater intrusion. The Hazard Index revealed a 45 % risk of health injury from oral exposure and

* Corresponding author at: Department of Geosciences, Texas Tech University, 1200 Memorial Circle, Lubbock, TX 79409, USA.
E-mail address: chaoxu@ttu.edu (C. Xu).

https://doi.org/10.1016/j.scitotenv.2025.180640
Received 12 April 2025; Received in revised form 21 September 2025; Accepted 25 September 2025
Available online 10 October 2025
0048-9697/Published by Elsevier B.V.

a 65 % risk from dermal exposure, with specific risks for children identified as 45 % for dermal and 35 % for oral exposure. These findings underscore the critical impact of heavy metal contamination and seawater intrusion on groundwater quality, posing substantial health risks to coastal residents.

1. Introduction

Approximately half of the worldwide urban population depends on subterranean water supplies; nevertheless, human beings are contaminating and excessively using these resources, which might result in permanent ramifications (Sonet et al., 2025; Yu et al., 2025). Moreover, groundwater supplies 84 %, 44 %, and 63 % of daily water for households, manufacturing, and farming, yet contamination from heavy metal wastewater poses significant health risks due to population growth, urbanization, industrialization, excessive resource use, and land reclamation (Ahmed et al., 2019a; Chiamsathit et al., 2020; Liu et al., 2023). Taking Bangladesh as an example, particularly in Satkhira District, unplanned construction is leading to environmental challenges such as issues with water supply, sanitation, and urban flooding protection (Faruque et al., 2022). As a consequence, heavy metals like Iron (Fe), Arsenic (As), and Zinc (Zn) are significantly affecting ecological conditions, resulting in health problems such as cancer, hypertension, lung and vascular diseases, neurological disorders, and reproductive issues (Karim, 2011; Rahman et al., 2023). Moreover, studies by Tasnim et al. (2025), Ahmed et al. (2020a), and Saha et al. (2019) have shown that As pollution in water supply sources is increasing, thereby posing additional health risks to the coastal residents of Bangladesh. Specifically, Fe pollution can cause symptoms like weight loss, fatigue, joint pain, and unusual changes in water color. Meanwhile, Zn-contaminated water may lead to abdominal discomfort, nausea, and vomiting among the residents (Kavitha et al., 2019; Mahapatra et al., 2020). Furthermore, metal pollution impairs reproduction and increases illness risk in native species, leading to reduced species abundance and even extinction (Rakib et al., 2022; Zhang et al., 2016).

Bangladesh serves as a prime example of a developing country where urbanization heavily depends on groundwater and surface water, exacerbating groundwater contamination (Ahmed et al., 2021a; Hasan et al., 2020; Sarker et al., 2022a). While previous studies by Ahmed et al. (2019b), Ahmed et al. (2020b), and Rahman et al. (2023) have investigated water quality and heavy metal pollution, they lacked a comprehensive assessment of the impact of contaminated groundwater. Similarly, studies by Rahman et al. (2023) and Rakib et al. (2022) have indicated that the levels of various heavy metals, including Chromium (Cr), Manganese (Mn), Iron (Fe), Zinc (Zn), and Nickel (Ni) found in water, sediment, and fish across many coastal regions of Bangladesh exceed the allowable limits for human health, as shown by spatial autocorrelation. In response, Bodrud-Doza et al. (2019) employed various indices, such as the Heavy Metal Evaluation Index (HMEI), Degree of Contamination (C_d), Nemerov Pollution Index (NPI), and Heavy Metal Pollution Index (HMPI), to assess the total pollution and associated health risks in Damurhuda Upazila. However, the groundwater risk assessment for the coastal area remains unaddressed. As a result, the researchers discovered that around 40 %, 27 %, and 60 % of the samples, respectively had a moderate amount of contamination. On the other hand, Hasan et al. (2020) lack statistical assessment, such as Response Surface Methodology (RSM), to comprehensively analyze the environmental consequences of heavy metal contamination in groundwater. In addition, excessive intake of Cu, Zn, and Fe is detrimental for plants (Rakib et al., 2022; Siegel, 2002; Xue et al., 1993), which becomes a major concern of groundwater pollution regarding agricultural sustainability, especially in coastal areas. In response to this, an urgent task is to comprehensively assess the situation and come up with a reasonable management plan based upon, for example, RSM or Central Composite Design (CCD). Additionally, Ahmed et al. (2020a) and Jahin et al. (2020) noted the presence of high levels of arsenic and salinity in Jashore, Bangladesh, but did not provide comparisons with other heavy metals in this coastal area. Similarly, Ahmed et al. (2022) conducted an assessment of groundwater in the southwestern coastal part of Bangladesh, yet it lacked any mention of heavy metals or their health impacts on the coast. It has been acknowledged by Bhuiyan et al. (2016), Mahapatra et al. (2020), and Tasnim et al. (2025) have demonstrated that groundwater quality in Bangladesh's coastal areas is declining due to saline intrusion and higher levels of trace metals.

Hydrochemical pollutants, such as heavy metals, are significant contributors to environmental contamination. This is a major public health concern due to their ability to infiltrate and accumulate within food chains, ultimately causing substantial harm to the ecosystem in this coastal region (Bodrud-Doza et al., 2019; Jahin et al., 2020). Aside from knowledge gaps, we should also acknowledge that previous studies have successfully demonstrated how to use statistical indices and methods to systematically analyze and evaluate the level of heavy metal pollution. For example, Karim (2011), Nkpaa et al. (2018), and Wu et al. (1993) used NPI to analyze raw analytical datasets, as well as USEPA (2009) and USEPA (2004) used HMEI and HMPI to assess groundwater quality and evaluate human health risk. Moreover, Principal Component Analysis (PCA) was used to simplify and interpret complicated raw datasets of heavy metal Zakir et al. (2020), which can further identify heavy metal pollutants, assess contamination rates, and evaluate environmental consequences. Moreover, for multivariate statistical methods, Bodrud-Doza et al. (2019) have demonstrated powerful applications in extensive statistics: for example, reducing the abundance of variables and enabling the investigation of their relationships within a simple set. In particular, Wang et al. (2021) and Monir et al. (2021) have simulated various characterization variables using Design-Expert®, version 7 software (DX7), which contains an RSM feature. Specifically, Monir et al. (2021) used CCD and Analysis of Variance (ANOVA) to evaluate the accuracy of constructed predictive models. While there is great progress in hydrochemical assessment, it is far from meeting the practical needs of comprehensive management and control for heavy metal pollution, especially for larger areas.

The previous reconnaissance assessments indicated that concentrations of specific heavy metals, including arsenic (As), iron (Fe), and zinc (Zn), were relatively high in aquifers in certain coastal areas (Ahmed et al., 2020a; Ahmed et al., 2022; Rahman et al., 2020). Furthermore, numerous analyses have been conducted across various coastal regions of Bangladesh, revealing a range of concentrations of trace elements in aquifers and the related health risks (Ahmed et al., 2022; Datta et al., 2020; Kibria et al., 2016; Tasnim et al., 2025). This time, we are distinctive for its comprehensive examination of groundwater in coastal regions, encompassing hydrochemistry, heavy metals, and statistical analysis. It aims to provide vital information for decision-makers to enhance groundwater management and mitigate health hazards associated with pollution. Additionally, the research examines the correlation between groundwater quality and public health, specifically addressing health concerns related to heavy metals and other pollutants by employing World Health Organization (WHO) criteria and health indicators. Recognizing the progress and knowledge gaps in existing studies, this paper examines the exposure of adults and children to heavy metals through oral and dermal contact by utilizing groundwater samples from Satkhira District, while also acknowledging the achievements and limitations of previous studies. Specifically, we use multivariate statistics (PCA and correlation matrix) and pollution indices (HMEI, NPI, C_d, and HMPI) to assess the correlation between groundwater quality and health risks. In addition, we use CCD. to optimize independent variables of groundwater constituents, which statistically affect

sorption. Finally, we find optimum data models through index visualization, and the results are verified by ANOVA.

2. Study area

The Satkhira District (Fig. 1b) has an area of 3817 km^2, where the population density is 3500/km^2. Furthermore, Satkhira, the study area, together with Jashore, Narail, Khulna, and Bagerhat, are the five coastal districts that collectively consist of the southwestern coastline zone of Bangladesh (Fig. 1a). Overall, Satkhira District is featured by humid climate in summer and mild climate in winter: highest temperature ranges from 25.6 °C in February to 34.3 °C in May; by contrast, lowest temperature is about 26.2 °C in August to 12.4 °C in January. According to Rahman et al. (2016), the annual precipitation and evaporation in Kalaroa, the northernmost area of Satkhira District, typically range from 1300 to 1700 mm.

Several rivers pass through the Satkhira District, including but not limited to Morichap River, Kholpetua River, Betna River, Raimangal River, Hariabhanga River, Ichamati River, Betrabati River, Kalindi-Jamuna River, which makes a dense river and delta channel network (Fig. 1b). This region has plentiful surface water, yet 70 % of the population utilizes groundwater for home and agricultural usage. The research area, predominantly rural and reliant on agriculture, features a land use pattern where residential land accounts for 25 %. Forest or tree plantations constitute a modest 2 %, while water bodies occupy just 1 %. A significant water quality concern in this region is seawater intrusion, which poses a threat to groundwater resources. Geologically, Satkhira's coastal district is characterized by the extinct Holocene to Recent Alluvium and a tidal plain. This geological composition plays a crucial role in the area's hydrogeology and influences the occurrence and extent of seawater intrusion, making it a critical factor to consider in any assessment of groundwater quality and management strategies (Datta et al., 2020). According to Dola et al. (2018), this area is covered by sandy layers and features by litho-stratigraphic units. Overall, it is characterized by low elevation, intricate landscape, and a complex river process. The Meghna River contributes to the floodplain, while tertiary and quaternary sand types have a high content of clay (Sarker et al., 2022a).

3. Materials and method

In general, the workflow of this study is illustrated in Fig. 2, which consists of sampling and preparation (Section 3.1), analysis in the laboratory (Section 3.2), assessment of health hazards (Section 3.4), as well as statistical analysis (Section 3.5).

3.1. Groundwater sampling and preparation

Following the procedures outlined by previous studies (Ahmed et al., 2021b; Ahmed et al., 2022; Hasan et al., 2020), a total of 66 water samples were collected throughout Satkhira District (Fig. 1a, b) from January to June 2023. This comprehensive analysis was specifically conducted during this period to account for seasonal fluctuations, monsoon run-off, droughts, farming conditions, temperature variations, precipitation, groundwater recharge, and changes in water quality and contaminant levels. All samples were collected from the open-handed-dug wells and boreholes, which were used to estimate hydrochemical properties and heavy metals. Additionally, to collect groundwater samples and conduct numerous analytical hydrochemical tests, 500 mL high-density FEP/PTFE (fluorinated ethylene propylene/Teflon) bottles were utilized based on ISO (2009), APHA (2023), and ISO (2023) guidelines. After collection, all samples were immediately preserved and

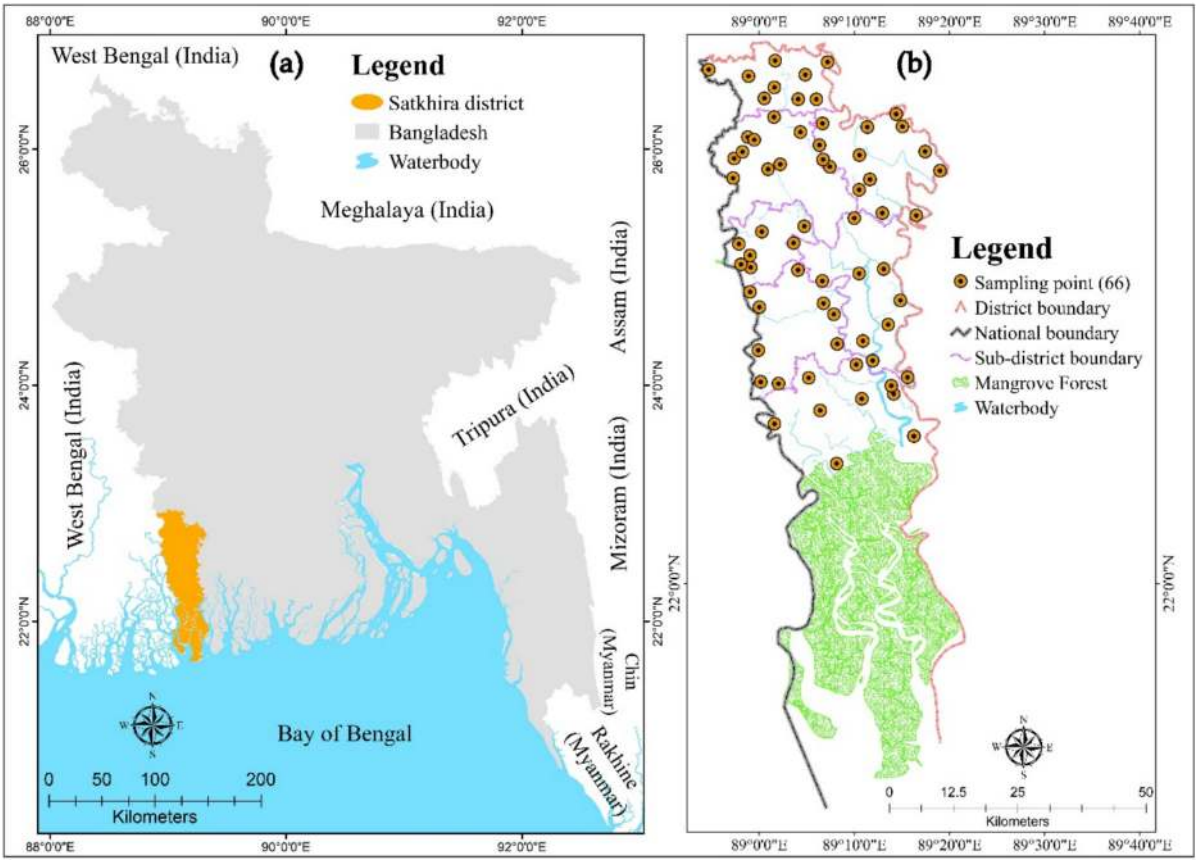

Fig. 1. A clear visual representation of the study area, highlighting both the (a) geographical context of Satkhira District within the People's Republic of Bangladesh and (b) specific locations of the sampling sites within the district.

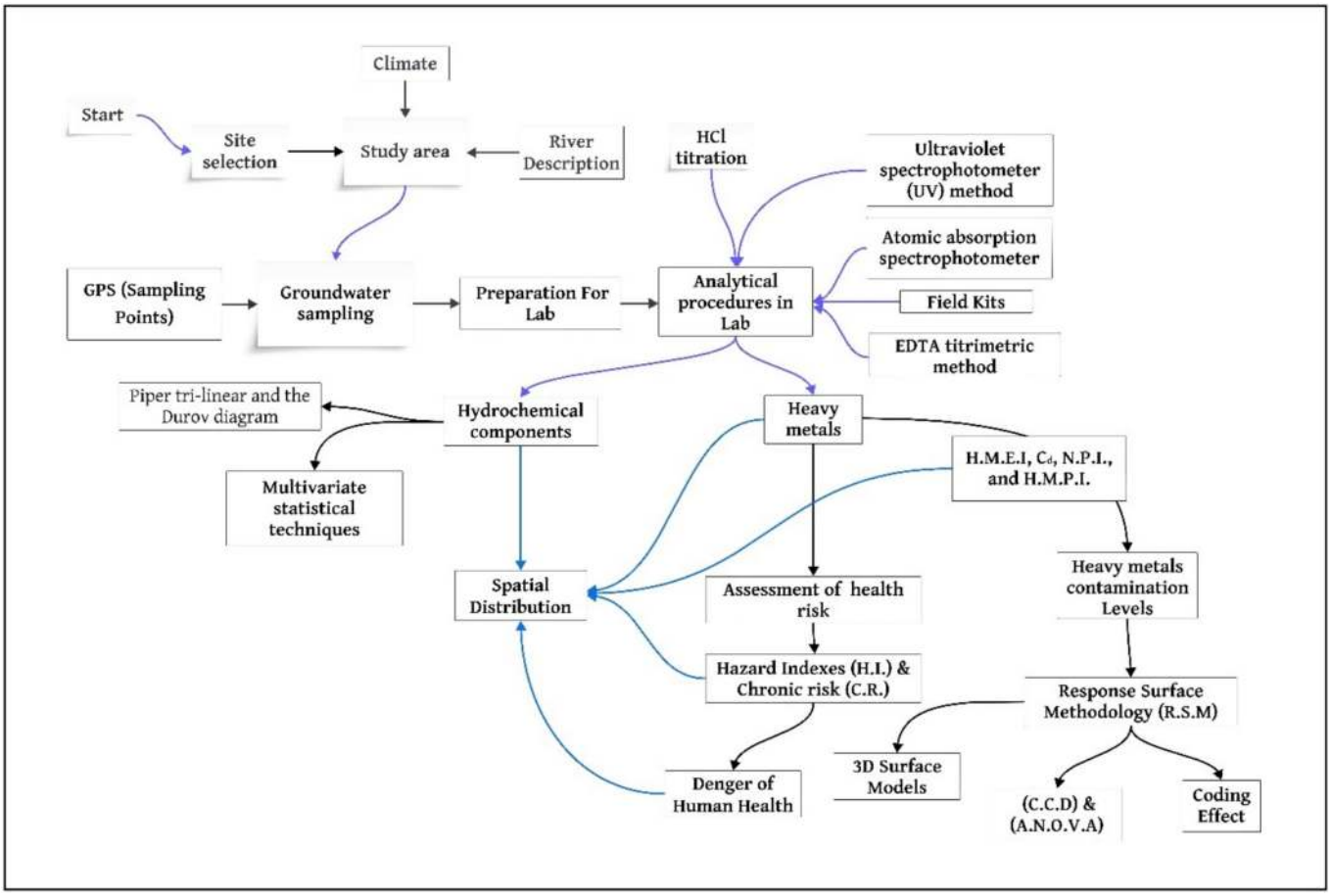

Fig. 2. The overall flowchart illustrating data collection and analysis for this study.

stored in temperature-controlled insulated containers at ≤4 °C throughout field collection, transportation, and until laboratory analysis, adhering to Standard Methods of APHA (2023). To ensure cleanliness and prevent organic growth, all bottles were cleaned with a 1:1 mixture of nitric acid (HNO_3) (Ahmed et al., 2022; Rahman et al., 2023; Tasnim et al., 2025). According to standard protocols from APHA (2023), ISO (2009), and ISO (2023), the procedures for sample collection, preservation, and analysis have been meticulously maintained. Specifically, bottles were washed with DI water to prepare for groundwater sampling. Additionally, all samples were collected separately for heavy metals and hydrochemical analytical tests in the laboratory to maintain the sensitivity of heavy metals, ensure proper handling (APHA, 2023), and adhere to Standard Methods of APHA (2023) to prevent contamination, ensuring accurate field sampling identification. Last but not least, every borehole sampling point's geographic coordinate (Fig. 1b), as well as the elevation, has been measured and recorded by a Garmin GPS handheld device (eXplorist 200) (Hasan et al., 2020). As a result, we found the bore log depths of these sample points vary from 250 to 300 ft., which falls in a moderate level (Ahmed et al., 2020b).

3.2. Analysis of physicochemical parameters in the laboratory

Once the samples were collected from the study area, they were transported to the Bangladesh Agricultural Development Corporation (BADC) laboratory in Chanchra, Jashore District, where all components of the groundwater were meticulously measured. To ensure the accuracy of the laboratory analyses, we adhered to the methods outlined in Table S1 and followed the guidelines from previous studies (Ahmed et al., 2020a; Mahapatra et al., 2020).

3.3. Pollution evaluation metrics

The pollution evaluation indices, which are based on the concentration of heavy metals in water, have proven to be highly effective for assessing the quality of water bodies. These indices provide a comprehensive representation of the cumulative impact of various dissolved heavy metals originating from the surrounding environment. Furthermore, HMEI, C_d, NPI, and HMPI have been evaluated to identify groundwater quality in the investigated area.

The HMEI reveals important information about the groundwater's overall quality concerning the presence of trace metals, as noted by Edet and Offiong (2002). The calculation of HMEI is as follows:

$$\mathrm{HMEI} = \sum_{i=1}^{n} \frac{H_c}{H_{mac}} \tag{1}$$

where H_c is the monitoring value and H_{mac} is the maximum allowable concentration (MAC) of the ith value. The classification is as follows: Low if the index is not greater than 10, Medium if greater than 10 and less than 20, and High if not less than 20 (Ahmed et al., 2019c; Edet and Offiong, 2002).

The (C_d) is determined by the quality of each contaminant or water quality parameter and is calculated using the equation from (Backman and Mackie, 1997):

$$C_d = \sum_{i=1}^{n} C_{ft} \tag{2}$$

where $C_{ft} = \frac{C_{Ai}}{C_{Ni}}$ -1, with C_{ft} being the Contamination factor, C_{Ai} the analytical grade of the ith material, and C_{Ni} the normal concentration.

The classification is as follows: Low: less than 1; Medium: between 1 and 3; High: greater than 3.

The inspection reveals how heavy metals impact areas through NPI sources, calculated as:

$$NPI = \sqrt{\left(\frac{\left[\left(\frac{1}{n}\right)\sum\left(\frac{C_i}{S_i}\right)^2 + max\sum\left(\frac{C_i}{S_i}\right)^2\right]}{2}\right)} \quad (3)$$

where n is the number of indices, C_i is the measured content of heavy metal concentration, S_i is the standard ratio of selected amounts. The pollution levels are classified as: No pollution: less than 0.5; Clean: between 0.5 and 0.7; Warning: between 0.7 and 1; Polluted: between 1 and 2; Medium polluted: between 2 and 3; Severely polluted: greater than 3.

The simultaneous equation used to calculate the HMPI is:

$$\text{HMPI} = \frac{\sum_{i=1}^{n} W_i Q_i}{\sum_{i=1}^{n} W_i} \quad (4)$$

where Q_i is the quotient of the ith identified parameter and W_i is the weighted total of the temperature coefficient, with n being the number of features included in the computation. Q_i is determined as:

$$Q_I = \sum_{i=1}^{n} \frac{|M_i - I_i|}{S_i - I_i} \quad (5)$$

Here, M_i denotes the monitoring metal ions, and I_i and S_i are the idealized and conventional estimates of the ith parameter, respectively. The values for I_i are derived from the elements' MAC numbers, while S_i readings are derived from the Department of Energy's measured value (Standard, 1997). Non-contaminated water is classified as not greater than 100; contaminated water as greater than 100 (Edet and Offiong, 2002).

3.4. Assessment of chronic health risk

The characterization of potential risk category is often used as the foundation for determining if a heavy metal or metallic compound poses a carcinogenic or non-carcinogenic danger to human beings in the context of the health risk evaluation for each substance (USEPA, 2009). This study aims to assess non-cancer health risks associated with consuming freshwater and cutaneous contact with groundwater. It uses Hazard Quotients (HQ) and Hazard Indexes (HI) to evaluate exposure to heavy metals through water ingestion and dermal absorption. The primary mortality risk variables include the slope factor (SF) for carcinogenic risk identification and the reference dose (RfD) for non-carcinogen hazard evaluation. The target population includes adults and children (Table S2). During evaluation, two different oral and dermal exposure routes were taken into account, and the chronic daily intake (CDI) of the substances through the oral and dermal routes was determined using the procedures outlined in the subsequent paragraphs (Bodrud-Doza et al., 2019; USEPA, 2004; Zakir et al., 2020). Initially, the CDIs of substances by consumption and dermal adsorption of drinks to human beings was determined by the following Eqs. (6) and (7), respectively, as defined by the United States Environmental Protection Agency (Bodrud-Doza et al., 2019; Karim, 2011; Sharmin et al., 2020; USEPA, 2004).

$$CDI_{Oral\left(mgkg^{-1}day^{-1}\right)} = \frac{(CW*ABS*IR*EF*ED)}{(BW*AT)} \quad (6)$$

$$CDI_{Dermal\left(mgkg^{-1}day^{-1}\right)} = \frac{(CW*ABS*SA*K_p*ET*EF*ED*CF)}{(BW*AT)} \quad (7)$$

where CDI_{Oral} and CDI_{Dermal} designate the exposure dosage (mg/kg/day) received via oral intake and dermal absorption, respectively, and are calculated using the values listed in Table S2.

The HQ is the proportion of the computed mean CDI of particular heavy metals to the oral (RfD) for the same heavy metal. This proportion is known as the heavy metal hazard ratio. The HQ of heavy metal from ingesting and dermal adsorption of fresh water to the population of the region was determined by applying the two equations below, (8) and (9), respectively (Gao et al., 2021; USEPA, 2004).

$$HQ_{oral} = \frac{CDI_{Oral}}{RfD_{Oral}} \quad (8)$$

$$HQ_{Dermal} = \frac{CDI_{Dermal}}{RfD_{Dermal}} \quad (9)$$

The H·I is the overall potential threat to health that is not responsible for cancer from the various heavy metals found in waterways. In addition, it was computed following the USEPA (2009) for the ingestion and dermal absorption of fluids by the persons living in the study area using Eqs. (10) and (11), respectively.

$$HI_{Oral} = \sum_{i=1}^{n} HQ_{Zn} + HQ_{As} + HQ_{Fe} \quad (10)$$

$$HI_{Dermal} = \sum_{i=1}^{n} HQ_{Zn} + HQ_{As} + HQ_{Fe} \quad (11)$$

The threshold of 1.0 to assess the potential non-carcinogenic health hazards from heavy metals in waterways. If the HI is less than 1.0, exposure to these metals is unlikely, while if it equals or exceeds 1, it suggests potential exposure to non-carcinogenic health hazards.

3.5. Tools for statistical analysis

The groundwater heavy metal data were analyzed utilizing multivariate statistical techniques, including PCA (Pearson, 1901), with the assistance of Minitab version 19 (Mahapatra et al., 2020). Also, Ordinary Kriging (Gao et al., 2021) module in ArcGIS 10.5 was utilized for the interpolation process. The hydrochemical investigation was shown graphically using the Piper tri-linear and the Durov diagram by AqQA version 19 (Chakraborty et al., 2014; Kavitha et al., 2019; Najafpour et al., 2020). Lastly, Design-Expert 7.1.6 was used to implement RSM (Kavitha et al., 2019; Monir et al., 2021), which identifies optimal conditions for an experiment with a control group.

4. Results and discussion

4.1. General statistics of aquifer hydrochemistry

This research aims to closely examine the distribution of As, Fe, and Zn in this coastal district, considering pollution sources, water chemistry studies, and potential health impacts on the population. The tests on groundwater samples yielded significant results, as shown in Table 3S(a) and Fig. 3(a, b & c), which present the levels of major cations and anions in the order they appear. The observed order of cation concentrations was: $Na^+ > Mg^{2+} > Ca^{2+} > K^+$. In contrast, the anion concentrations followed a different hierarchy: $Cl^- > HCO_3^- > SO_4^{2-} > CO_3^{2-}$. This sequence highlights the differential mobilization and solubility of these ions within the aquifer system.

The increase in TDS, along with other major cations and anions, suggests that seawater is infiltrating the well or nearby areas. This infiltration impacts not only the coastline but also more distant regions (Kanagaraj et al., 2018). In the study area, TDS levels range from 408.281 mg/L to 21,353.123 mg/L, with an average of 10,913.534 mg/L. TDS and EC levels are notably high in coastal cities such as Bagerhat and Barishal–Chandpur (Bodrud-Doza et al., 2019; Mahapatra et al.,

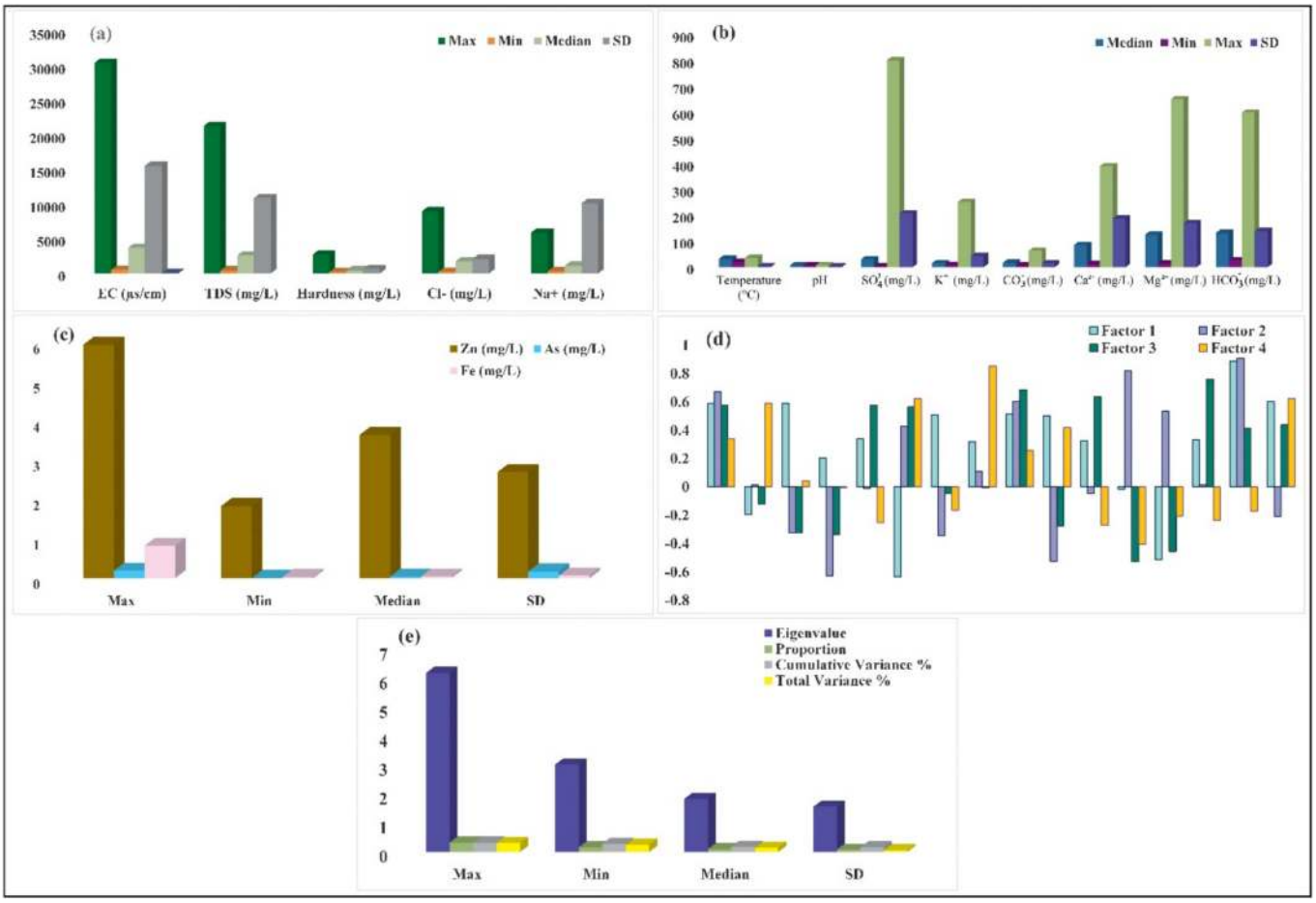

Fig. 3. Statistical summary of heavy metals and groundwater components in the study; (a) and (b) Water components; (c) heavy metals; (d) Factor analysis of Components; (e) Initial eigenvalues.

2020) and this study area also located within this same coastal aquifer region. Across the entire area, EC ranges from 518.234 µs/cm to 30,503.890 µs/cm, with an average of 15,590.134 µs/cm, as shown in Fig. 3(a) and Table 3S(a). According to USEPA (2004)), the permissible level for hardness in water consumed in Bangladesh is set at 500 mg/L. The analysis indicates that 64 % of the water samples exceed this standard, posing a health hazard for human consumption.

We noted that 68 % of samples displayed Ca^{2+} and Mg^{2+} levels exceeding standards. Additionally, the ion concentrations in the aquifers were, on average, more pronounced than those reported in previous studies conducted in coastal Bangladesh. Furthermore, 54 % of freshwater samples exhibit K^{+} levels that surpass World Health Organization thresholds (USEPA, 2009), rendering them unsuitable for consumption. This issue arises from unique coastal water conditions that make access to mineral-rich sources challenging. Consequently, groundwater exhibits high Na^{+} and moderate K^{+} levels. The cation exchange process increases Na^{+} levels by swapping Ca^{2+} ions for other cations that bind to clay in the soil, thereby altering the composition of groundwater. According to Bodrud-Doza et al. (2019), elevated Na^{+} levels in freshwater ecosystems initiate a breakdown process that disrupts the balance of various elements, resulting in their deterioration and disintegration.

Another study by Rahman et al. (2016) has demonstrated that these water sources predominantly originate from sedimentary rocks, such as sandstone and mudstone, which contain sodium at concentrations that dissolve readily upon contact with water. Additionally, groundwater HCO_3^{-} levels varied from 133.265 to 599.822 mg/L, with a median of 139.856 mg/L. According to Fig. 3b and Table 3S(a), 45 % of groundwater samples exhibited CO_3^{-} levels exceeding the upper limit. Furthermore, higher levels of HCO_3^{-} have been found in the coastal and surrounding areas. Some studies suggest that elevated HCO_3^{-} levels arise from reactions between carbon dioxide in the soil and silicate minerals, which produce H_2CO_3 (Wang et al., 2021; Zakir et al., 2020). Another research by Karim (2011) and Rakib et al. (2022) indicates that areas with higher HCO_3^{-} levels in groundwater suggest that silica and carbonates have broken down from various types of rocks in the region being studied.

4.2. Spatial distribution

4.2.1. Major hydro-components

Previous research conducted along the northwestern coast of Bangladesh indicated a range akin to that of this study (Tasnim et al., 2025; Zakir et al., 2020; Zhang et al., 2016). Also, Table 3S(a) outlines the groundwater safety parameters for consumption as set by the USEPA (2009). Consequently, all groundwater samples were classified as non-compliant with these standards. The analysis revealed the water quality as follows: 31 % 'Good', 19 % 'Permissible', 11 % 'Doubtful', and 41 % 'Not acceptable' (Fig. 4b). This finding suggests that regions with suitable drinking water have experienced an increase in saline intrusion, aligning with the findings of Shi and Jiao (2014) and Siegel (2002). Then, EC measurements ranged from 518.024 µS/cm to 30,503.123 µS/cm, with an average of 3693.833 µS/cm and a standard deviation of 15,590.142 µS/cm Fig. 3a and Table 3S(a). Variations in EC reflect differing levels of ionization and dissolved particles in the groundwater samples. Notably, groundwater with higher ion concentrations typically exhibits superior EC values, reflecting increased electrical conductance

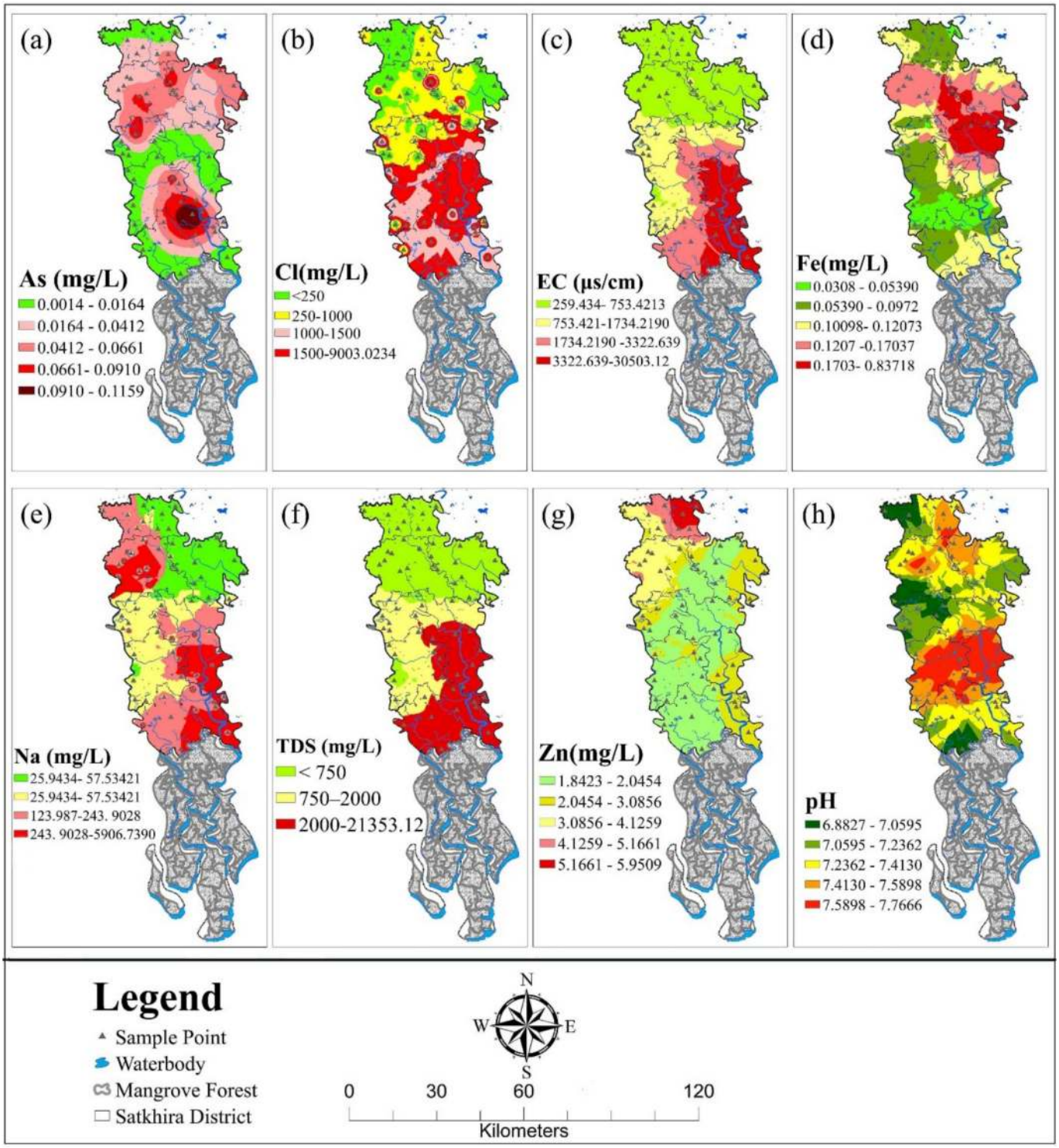

Fig. 4. The spatial distribution of heavy metals and other key components identified from groundwater in the study area, including (a) As, (b) Cl, (c) EC, (d) Fe, (e) Na, (f) TDS, (g) Zn, and (h) pH.

due to the presence of more charged particles (Ahmed et al., 2020b). According to USEPA (2009), the study area is classified as follows in Fig. 4c: 43 % as 'Excellent', 19 % as 'Good', 9 % as 'Permissible', and 29 % as 'Doubtful', respectively. In addition, EC is generally regarded as one of the most important criteria that may be used to categorize water safety for consumption (Sarker et al., 2022b; Sharmin et al., 2020).

In addition, Fig. 4e illustrates the geographical distribution of Na^+ values, which have been categorized into four distinct classifications: 36 % as 'Good', 19 % as 'Permissible', 22 % as 'Unsuitable', and 23 % as 'Not acceptable'. Also, Table 3S(a) reveals that the dataset spans a maximum concentration of 5906.731 mg/L, with the minimum recorded at 125.942 mg/L. The median value stands at 1093.834 mg/L, while the standard deviation measures 10,145 mg/L, Fig. 3(a) and Table 3S(a). Notably, Na^+ levels in coastal groundwater exceed potability thresholds, rendering it unsuitable for human consumption, following Sarker et al. (2022b). According to USEPA (2009), the standards governing water for drinking use stipulate that the maximum TDS level in water should not exceed 500 mg/L. Also, evaluated against this standard, all samples

were deemed safe for human consumption. Fig. 4f shows TDS levels, with 43 % classified as 'Good', 28 % as 'Permissible', and 29 % as 'Unsuitable' based on concentration. The dataset for these values spans from a low of 408.228 mg/L to a high of 21,353.122 mg/L, with a median at 2586.523 mg/L, and exhibits a standard deviation of 10,145.871 mg/L, Fig. 3(a) and Table 3S(a). Additionally, this statistical profile aligns closely with findings reported for the majority of coastal regions in Bangladesh (Rahman et al., 2023). 36.623 % of the samples in this research region exhibited that those samples crossed the limit of (pH < 6.50), which shows the acid-type characteristic.

Furthermore, according to Sharmin et al. (2020), presence of calcium, magnesium, and sodium in water significantly impacts the water's pH level. The pH values of the groundwater samples analyzed in this study exhibited a range from 6.314 to 8.472, with an average value of 7.121 and a standard deviation of 2.145 (Fig. 3(b) and Table 3S(a). Notably, an additional 64 % of the samples collected from subterranean sources indicated that the groundwater possesses alkaline characteristics, as illustrated in Fig. 4h. This finding indicates a significant prevalence of alkalinity in the groundwater samples, with implications for environmental and geological studies on subsurface water quality. Additionally, weathering, rock and soil degradation, and municipal pollutants contribute to highly dissolved sodium-potassium minerals. This phenomenon subsequently leads to a substantial increase in the concentration of NaCl within groundwater sources (Dola et al., 2018; Sharmin et al., 2020). In addition, leaching of higher soils by pollutants from homes, municipalities, and industry and dry climatic conditions may also increase groundwater Cl^- concentrations (Datta et al., 2020; Wang et al., 2021). According to Gao et al. (2021), higher concentrations of Na^+ and Cl^- imply that the groundwater may have a greater concentration and maximum ionic activity due to massive saltwater intrusion.

4.2.2. Heavy metal contamination

The concentration levels of As in groundwater exhibit a significant range, from a minimal value of 0.001 mg/L to a notably elevated level of 0.056 mg/L. Statistical analysis reveals a median As concentration of 0.039 mg/L, with a standard deviation of 0.171 mg/L (Fig. 3(c) and Table 3S(a)). Furthermore, Fig. 4a indicates that 45 % of the samples exceed the allowed limits. In contrast to findings by our peers (Ahmed et al., 2020a; Hasan et al., 2020), our research highlights a widespread increase in elevated As levels across the surrounding areas, emphasizing an environmental concern that requires further investigation and potential remediation efforts.

In the examined region, the concentrations of Fe in groundwater samples varied between 0.032 and 0.825 mg/L, with a mean value of 0.039 mg/L and a standard deviation of 0.066 mg/L (Fig. 3(c) and Table 3S(a)). Approximately 25 % of the analyzed samples exceeded the regulatory thresholds set by the USEPA (2009) for permissible levels of Fe in drinking water. Alarmingly, Fig. 4d shows that 65 % of these samples exhibit Fe levels surpassing acceptable drinking water quality standards. Numerous studies (Karim, 2011; Zakir et al., 2020) have demonstrated that Fe occurs naturally in various water sources, including surface and groundwater. However, large amounts of Fe pollution have been detected in these coastal areas, as shown by Mahapatra et al. (2020). Prolonged consumption of water with high Fe content can be harmful to individuals of all age groups (Bodrud-Doza et al., 2019).

The observed concentrations of Zn in groundwater range from 1.844 mg/L to 5.952 mg/L. Statistical analysis reveals a standard deviation of 2.707 mg/L and an average concentration of 3.65 mg/L (Fig. 3(c) and Table 3S(a)). This level of Zn is relatively low compared to the concentrations of the other two metals examined. Geographically, the distribution patterns of these concentrations merit further investigation. Fig. 4g indicates that the aggregate quantity of Zn detected across all observation wells constitutes 31 % of the total, surpassing the safety threshold for potable water. This suggests that industrial manufacturing activities may influence Zn concentrations in groundwater, aligning with global studies (Ahmed et al., 2019a; Sarker et al., 2022a). Heavy metals pose a threat to ecosystems when found in large quantities, affecting people and natural processes such as substance breakdown, geothermal energy production, and rock saturation (Monir et al., 2021; Wang et al., 2021). According to Fig. 4(a, d & g), the trace metals are distributed in decreasing order: Zn > Fe > As.

4.3. Degree of contamination in groundwater

The HMEI was used to assess groundwater heavy metal levels and further identify and quantify groundwater quality trends (Singh et al., 2018). Among the 66 groundwater samples obtained from the Satkhira District, 44 % fall under the 'low effect' group, 30 % have been classified as 'medium effect', and the remaining 26 % were determined as 'high effect'. The geographical classification is shown in Fig. 5a, according to the estimated HMEI standards (Bodrud-Doza et al., 2019; Edet and Offiong, 2002). The figure suggests that heavy elements, including Zn, Fe, and As, in groundwater samples from certain places made the water unsuitable for consumption (Ahmed et al., 2020b).

We utilized the HMPI to assess freshwater heavy metal levels, a valuable method for identifying and evaluating changes in groundwater purity (Sharmin et al., 2020). Fig. 5b reveals that 68 % of the samples collected exceeded the drinking water limits established by Edet and Offiong (2002), indicating that only 32 % of the sites are currently suitable for drinking water. Furthermore, according to Sharmin et al. (2020), two-thirds of the sample sites near mangrove forests showed a high pollution index.

Following Bodrud-Doza et al. (2019), Sarker et al. (2022b), and Singh et al. (2018), we also used the NPI to quantify heavy metal pollution in the groundwater samples. Fig. 5c shows the distribution: 37 % of sampling sites are clean; 25 % are in a warning range; 12 % are slightly polluted; 19 % are significantly polluted; and 7 % are severely polluted. Bodrud-Doza et al. (2019) also highlighted the increased risk of corrosion due to heavy metal pollution in groundwater.

Finally, based on the classification analysis by Bodrud-Doza et al. (2019) and Edet and Offiong (2002), Fig. 5d illustrates the C_d pollution levels: 59 % slightly polluted, 22 % significantly polluted, and 19 % highly polluted. This indicates that the southern and western regions show moderate to high levels of heavy metal contamination.

4.4. Principal physicochemical features of groundwater

This study used water chemistry data shown in Piper (1944) and Durov (1948) diagrams to determine the conditions of the aquifer. Likewise, the rationale behind using such graphical representations is substantiated by the scholarly works of Rahman et al. (2023) and the foundational study by Piper (1944).

The Piper diagram facilitated the analysis of Satkhira's aquifer, underscoring its water quality. Fig. 6c illustrates saline waters significantly affecting the Na—Cl facies in most samples. Notably, the Ca-Mg-HCO_3, Na—Cl, and Na-HCO_3 facies were present, while no Ca-Mg-SO_4 facies were detected, emphasizing the predominance of other facies types in the aquifer system. The cation triangle analysis identifies 94 % of freshwater resources as "Na-type", according to Fig. 6c. Conversely, the anion triangle shows that 6 % of groundwater samples are 'HCO_3-type,' 3 % have 'no prevailing type,' and 91 % are 'Cl-type.' The water samples revealed that 75.55 % had high sodium (Na^+) concentrations. Approximately 18 % of the samples were potable, with no dominant ionic composition. Additionally, 6.45 % were categorized as mixed water (SO_4^{2-} + Cl^-), with more alkaline earth metals (Ca^{2+} + Mg^{2+}) than alkalis (Na^+).

The Durov diagram, introduced by Durov (1948), is a valuable tool for understanding the complex hydro-geochemical characteristics of groundwater. This diagram helps to identify distinct water types, such as Mg–HCO_3 and Na–HCO_3 waters, corresponding to Zone 2 and Zone 3,

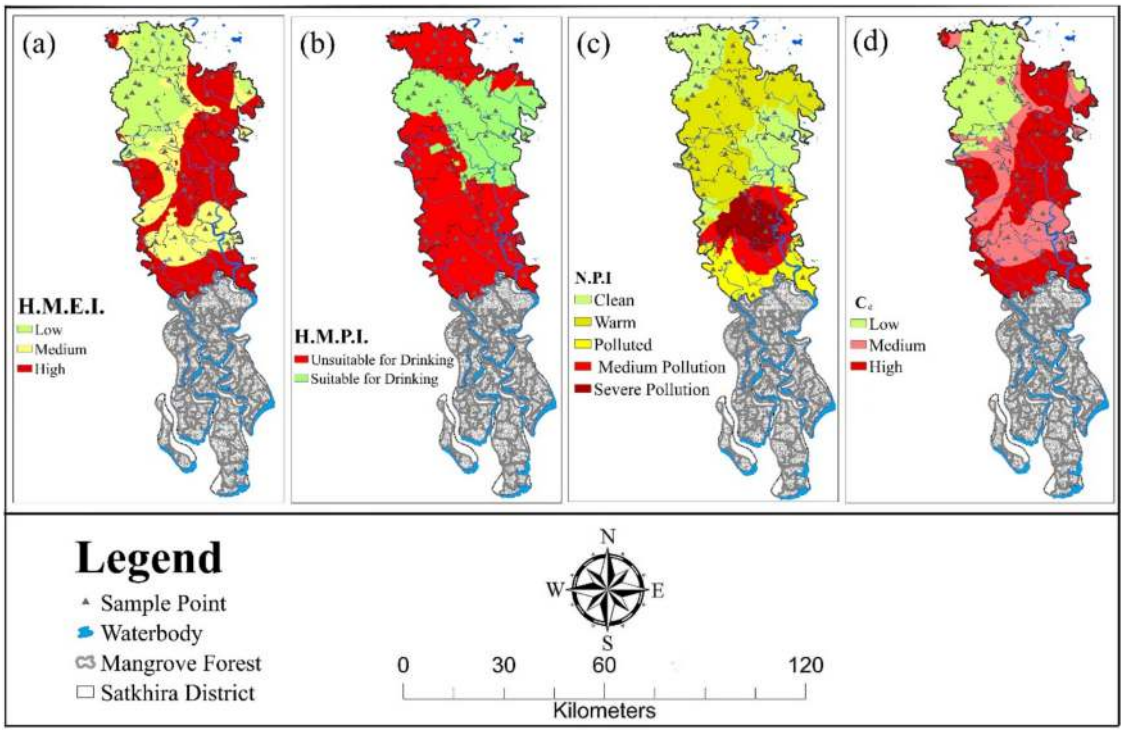

Fig. 5. The spatial pattern of heavy metals pollution evaluated by (a) HMEI, (b) HMPI, (c) NPI, and (d) C_d.

respectively. These zones represent key stages in the evolution of water chemistry, ultimately leading to Na—Cl water becoming the dominant type through a process known as reverse ion exchange. The sequential geochemical transformations within subsurface environments are highlighted by this comprehensive model.

Analysis of the groundwater samples using Durov's diagram reveals that a significant majority (86 %) fall within Zone 1, characterized by reverse ion exchange processes. The predominant water type in this zone is Ca–HCO_3, suggesting a potential origin from Mg–HCO_3 recharge waters (as evidenced by the 8 % of samples in Field No. 2 exhibiting this characteristic). Another smaller subset of samples (6 %) shows evidence of reversible ion exchange reactions in Zone 3, a phenomenon illustrated in Fig. 6c and d, which indicate mixing with seawater. Studies in the areas surrounding Satkhira, including Bagerhat and Jashore, reveal similar hydrogeochemical characteristics, further supported by the work of Bhuiyan et al. (2016), Rahman et al. (2020), and Rakib et al. (2022).

4.5. Statistical approach for evaluation

This section employs PCA and factor correlation coefficients to identify aquifer sources. This approach helps to assess significant positive and negative relationships between various hydrogeochemical parameters (Ahmed et al., 2021b; Ahmed et al., 2022; Bhuiyan et al., 2016).

4.5.1. Potential sources of heavy metals

Determining the sources of heavy metals in groundwater is crucial for mitigating future contamination, which can originate from natural or human activities (Bayuo et al., 2019; Bodrud-Doza et al., 2019). Also, natural and anthropogenic factors influence groundwater in the area. Analysis of groundwater samples identified four main factors (PC1–4) causing variations in the data (Table 3S(b)).

The eigenvalues for the four-factor components ranged from 6.204 to 1.565, reflecting the variance explained by each. The proportion of variance explained varied from 0.327 to 0.082, with total variance ranging from 0.327 to 0.165 (Table 3S(b)). Four parameters demonstrated a cumulative variance of 96 %, indicating they accounted for 96 % of the total variability in the groundwater sample. The total variance explained by the four-factor components was 78 %, capturing a substantial portion of the overall variance (Table 3S(c)). These results suggest that factors (PC1–4) effectively summaries the variability in the groundwater data, revealing the underlying causes of heavy metal contamination. Accordingly, we highlight several key points. In addition, factor 1 shows the highest variation, with a cumulative variation percentage of 0.327 and a total variance percentage of 0.316. Also, Fe has a significant negative loading, suggesting it does not contribute to the presence of heavy metals like Zn and As (Ahmed et al., 2021). Due to the coastal location, groundwater is contaminated with saltwater, introducing heavy metals like Fe, Cl, and EC (Ahmed et al., 2020b; Vetrimurugan et al., 2017).

Several factors contribute to heavy metal contamination in the groundwater. Manufacturing plants along riverbanks contribute through direct and indirect leaching (Ahmed et al., 2020a; Ahmed et al., 2019c). Fertilizers used in agriculture, particularly those containing phosphates, are significant sources of As and Zn, leaching into groundwater (Kibria et al., 2016; Rahman et al., 2020). Coastal hydrochemical processes, deriving from silt and rock layers, also introduce heavy metals into the aquifer (Ahmed et al., 2021b). Furthermore, erosion and weathering, exacerbated by construction, fertilizers, herbicides, and pesticides, contribute to the enrichment of heavy metals in groundwater (Bayuo et al., 2019; Bodrud-Doza et al., 2019). Farming practices, household waste, and chemical weathering also release As into the environment (Ahmed et al., 2020b; Vetrimurugan et al., 2017). Industrial waste dumping introduces additional heavy metals into the groundwater, impacting industries such as sugar, paper, textiles, cement, electroplating, paint, and mineral and metal processing (Ahmed et al., 2020a; Ahmed et al., 2022).

Seawater intrusion poses another significant threat, necessitating regulated pumping and integrated surface and groundwater use to prevent salinization (Rahman et al., 2023). Effective monitoring and management of groundwater resources are crucial for meeting local demands for drinking, residential, and agricultural purposes, while also

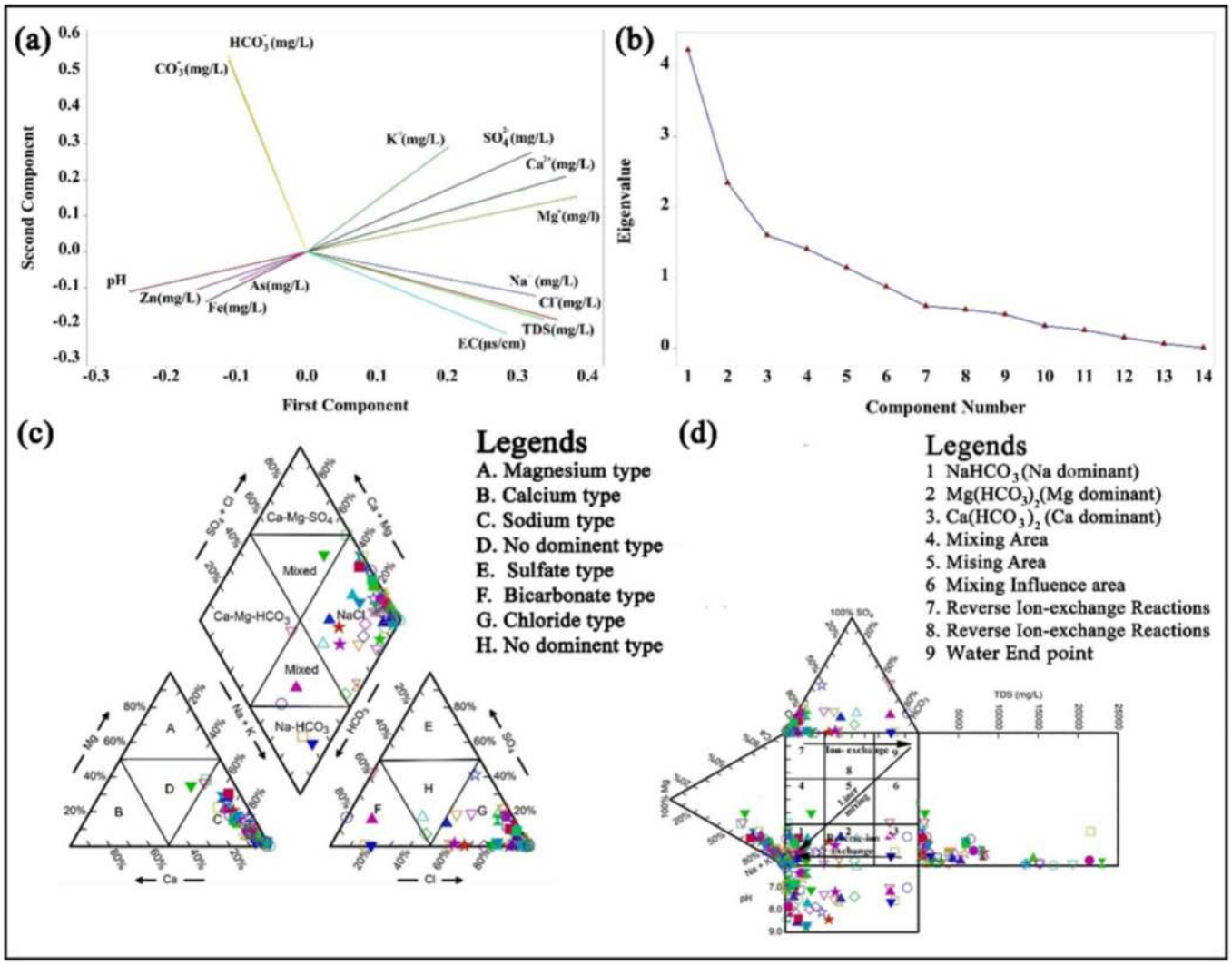

Fig. 6. The groundwater sample contents visualized by (a) component plots on a circular basis, (b) screen plots with distinctive roots (eigenvalues), (c) Piper, and (d) Durov diagrams.

mitigating the impact of contaminants (Rahman et al., 2023; Sharmin et al., 2020).

4.5.2. PCA analysis

PCA was employed to elucidate the clustering characteristics within the groundwater sample data and to assess the influence of variables such as Zn, Fe, and As on the overall data variation (Pearson, 1901; Rakib et al., 2022). The principal components (PCs) derived from the PCA were primarily driven by Zn and Fe, not As, suggesting that Zn and Fe are the main contributors to the variation observed in the groundwater data. The number of PCs retained was determined using the eigenvalue criterion (>1), with eigenvalues indicating the variance explained by each PC. Factor loadings, representing the strength of the relationship between original variables (Zn, Fe, As) and PCs, were interpreted as follows: below 0.5 indicates low load; 0.5 represents moderate load; and above 0.5 signifies high load (Ahmed et al., 2021b; Ahmed et al., 2022).

Correlation analysis (Pearson, 1901) revealed significant positive associations between TDS, CO_3^{2-}, and Mg^{2+} in the groundwater (Table S4). Additionally, these positive high correlation coefficients indicate a strong relationship, potentially linked to seawater intrusion, a phenomenon where salty water mixes with inland groundwater due to coastal hydrodynamic changes (Hasan et al., 2020; Rakib et al., 2022), which is also illustrated in Fig. 6 (b, c). This intrusion leads to increased levels of TDS, Na^+, EC, and Cl^- in the groundwater. Significant correlations (coefficients >0.5) were also observed between TDS, Cl^-, As, and Na^+, further supporting the impact of seawater intrusion. Additionally, Fe showed significant correlations with both As and Zn, highlighting the interconnectedness of these elements in the groundwater system.

Previous studies (Ahmed et al., 2020a; Bodrud-Doza et al., 2019) have shown that significant positive correlations between metals often indicate anthropogenic sources. The strong relationships between Zn, Fe, and As, along with their correlation with Cl^- and Na^+, suggest a common origin, such as industrial waste and inadequate wastewater management (Najafpour et al., 2020; Zakir et al., 2020). Silt and rock layers are significant sources of specific heavy metals (Mahapatra et al., 2020) and As and Zn are absorbed into groundwater through erosion (Ahmed et al., 2020b) and weathering processes influenced by human activities (Bodrud-Doza et al., 2019; Chiamsathit et al., 2020). The high Zn levels may also be influenced by chelating properties in the aquifer watershed. Conversely, Fe, abundant in the Earth's crust (Xue et al., 1993), appears to be primarily geological in origin (Ahmed et al., 2020a; Zakir et al., 2020).

Rotation of the first four principal components explains approximately 71.061 % of the total variance, with PC1, PC2, PC3, and PC4 accounting for 31.651 %, 25.512 %, 15.141 %, and 6.301 %, respectively (Table 3S(b) and (c)). Fig. 6a displays a loading plot, illustrating the relationships among parameters. A scree plot (Fig. 6b) shows the

eigenvalue proportions, where a sharp change indicates differences in plot gradients. The angle shifts from high to low after the first two components, with all eigenvalues from Factor 1 to Factor 3 being less than 1; thus, a solution using four variables (total variance 78 %, cumulative variance 96 %) is optimal for our study area. The proximity of these boundaries correlates strongly with local groundwater conditions (Bhuiyan et al., 2016; Bodrud-Doza et al., 2019).

4.6. Evaluation of heavy metal index by RSM

4.6.1. Evaluation of data and CCD modeling and ANOVA

The CCD with a quadratic structure was employed to elucidate the relationship between the ANOVA response and independent factors. This design investigated the impact of six key production factors (A, B, C, D, E, and F) on groundwater levels of three ions (As, Fe, and Zn) and three other compounds (TDS, pH, and EC), assessed using four indices (C_d, HMPI, NPI, and HMEI). Tables S5 and S6 present the CCD design matrix and resulting ANOVA results. The index evaluations were based on experimental data.

Model development involved identifying significant model components through analysis of the coded variables. The following components were found to be significant: AB, AC, AD, AE, AF, BC, BD, BE, BF, CD, CE, CF, DE, DF, EF, A^2, B^2, C^2, D^2, E^2, and F^2. These results highlight the importance of each variable in forming hydrochemical compounds, supporting prior research on heavy metal indices. Four polynomial modeling equations (detailed in supplementary material) describe the effects of these factors on As, Fe, Zn, TDS, pH, and EC, along with associated categorized quantities. Second-order nematic equations (S1-S4) further illustrate how groundwater contamination increases the levels of these substances. The ANOVA results (Tables S5 and S6) are based on the optimized numerical values of these equations.

The agreement between expected and actual index values was strong, with minor discrepancies (Monir et al., 2021). The coefficient of determination (R^2) for the four indices are presented in Tables S5-S6: Cd (0.250), HMPI (0.344), NPI (0.225), and HMEI (0.284), supporting model adequacy. Tables S5(a) and (b) show that procedural variables account for 61.511 % and 62.041 % of the variance, while Tables S6(a) and (b) show variances of 119.511 % and 53.041 %, respectively. Notably, the heavy metal indices showed lower R^2 values, with the model explaining only 1.272 % of the variance in the observed response (Monir et al., 2021). Despite this, a minor loss of fit is considered acceptable given the aim for optimal fit (Barakat, 2011). A strong correlation is indicated by R^2 values between 0.751 and 0.9 (Monir et al., 2021). All models exhibited high R^2 values, ranging from 0.225 to 0.344. Adjusted R^2 values are also reported, indicating a strong relationship between actual and expected values.

ANOVA was used to assess model suitability by partitioning the total variance into model and residual components (Garba et al., 2016). The F-value was used to assess the significance of the model. F-values exceeding the critical F-value indicate that the model effectively explains the experimental results (Ani et al., 2015). The calculated F-values (Tables S5 and S6) suggest an adequate response from the field model. The significance of each variable was evaluated based on the probability of the error statistic (Prob > F). Values below 0.050 (Tables S5 and S6) indicate statistical significance. The three processing variables significantly affected the four main heavy metal indices. The 3D quadratic model with high heavy metal indices had F-values of 2.441 and 3.471 in Tables S5(a) and (b), and 2.221 and 6.152 in Tables S6(a) and (b), indicating a significant influence on the relationship with groundwater components (A) TDS, (B) EC, and (C) pH, and their combined effect on (D) As, (E) Fe, and (F) Zn. Only exponential impacts of groundwater were identified through the heavy metal indices. The lack of fit F-values suggest a comparison of lack of fit to pure error.

4.6.2. The sufficiency analysis of 3D surface models

This section assesses a mathematical model's effectiveness using six key factors: heavy metals (As, Fe, and Zn) and essential water chemistry elements (EC, pH, and TDS). Three-dimensional (3D) response surface graphs and diagnostic visuals evaluate model suitability. These results, calculated using eqs. (S1-S4), represent the first measurements of metal ion levels in these solutions. The model's predictions and the study's findings illustrate the relationships among these components using 3D plots, equations, and coded methods (Bayuo et al., 2019; Garba et al., 2016).

Fig. 7(a-f) numerically shows the coded impact of each metal ion. pH, TDS, and Fe show negative influences (−1, −0.946, and − 0.913, respectively), while EC, As, and Zn show positive impacts (0.865, 0.649, and 0.892, respectively). This indicates that salinity intrusion and heavy metals significantly affect groundwater in this region. Fig. 8(a-i) illustrates the correlation between heavy metals and key groundwater components in 3D plots. The NPI is the target variable; its strong connection with pH and other heavy metals is demonstrated by target responses (Fig. 8a-c)): $pH_{As} < pH_{Fe} < pH_{Zn}$. Similar trends are observed for EC and TDS (Fig. 8d-f and Fig. 8g-i). The increasing index at higher cycles may be attributed to the primary indexing factors (Ahmed et al., 2020a; Bodrud-Doza et al., 2019).

Fig. S1 (a-i) shows the relationship between heavy metals and critical components. The target response to C_d is illustrated in Fig. S1 (a-c), highlighting the correlation between pH and impactful heavy metals. Additionally, early in this process, there is a quick transition to maximum levels. The highest point is indicated by the ratio $EC_{As} > EC_{Fe} < EC_{Zn}$ (Fig. S1 a-c), with the optimal value for C_d identified as Sqrt(R) = 1.951 > 0.652 < 0.703. Furthermore, Fig. S1 (d-f) shows that $pH_{As} > pH_{Fe} < pH_{Zn}$. Based on these numerical valuations, the optimal ratios indicate Sqrt(R) = 1.853 > 0.653 < 0.704, which corresponds to EC_{C_d}. Additionally, Fig. S1 (g-i) shows that $TDS_{As} > TDS_{Fe} < TDS_{Zn}$, with values of 1.853 > 0.245 < 0.560.

Supplementary Figs. S1 and S2 illustrate the relationships between heavy metals and critical components for the C_d and HMEI, respectively. These figures show a rapid transition to maximum levels early in the process. Similar trends are observed for EC, pH, and TDS across all indices. Supplementary Fig. S3 shows the impact of heavy metals on the HPEI. The initial stages show a rapid transition from maximum to minimum values. Optimal maximization suggests greater seawater intrusion and higher heavy metal indices. Eqs. (S1-S4) demonstrate that heavy metal levels reduce groundwater quality. Rising indices may expand accessible surface areas and active sites, contributing to impactful groundwater development. These findings align with studies on heavy metal indices (Bayuo et al., 2019; Zakir et al., 2020; Zhang et al., 2016).

4.7. Human health hazards assessment

Groundwater in the study area is heavily contaminated with arsenic (As), zinc (Zn), and iron (Fe), which are associated with serious long-term health outcomes, including skin cancer (Zhang et al., 2016), bladder disease (Zakir et al., 2020), nausea (Singh et al., 2018), vomiting (Bodrud-Doza et al., 2019), diarrhea (Nkpaa et al., 2018), liver cirrhosis (Rahman et al., 2016), heart failure (Rakib et al., 2022), and hemochromatosis due to chronic Fe over-intake (Sharmin et al., 2020). We conducted a human health risk assessment (HRA) following the widely adopted U.S. Environmental Protection Agency (U.S. EPA, 2009) methodology. These health effects arise primarily with prolonged ingestion of water contaminated by heavy metals (As, Zn, Fe), and such pollution is increasingly reported in Bangladesh, China, and Iran (Bodrud-Doza et al., 2019; Wang et al., 2021; Zhang et al., 2016). Prior studies indicate that As poses the greatest risk in this coastal region, exceeding risks from Zn and Fe (Hasan et al., 2020; Karim, 2011).

The HRA framework provides a geospatial depiction of health risks from groundwater contamination (Sarker et al., 2022a; Wang et al., 2021). We evaluated both exposure pathways—oral ingestion and dermal contact—and quantified non-carcinogenic HQ, HI, and CR.

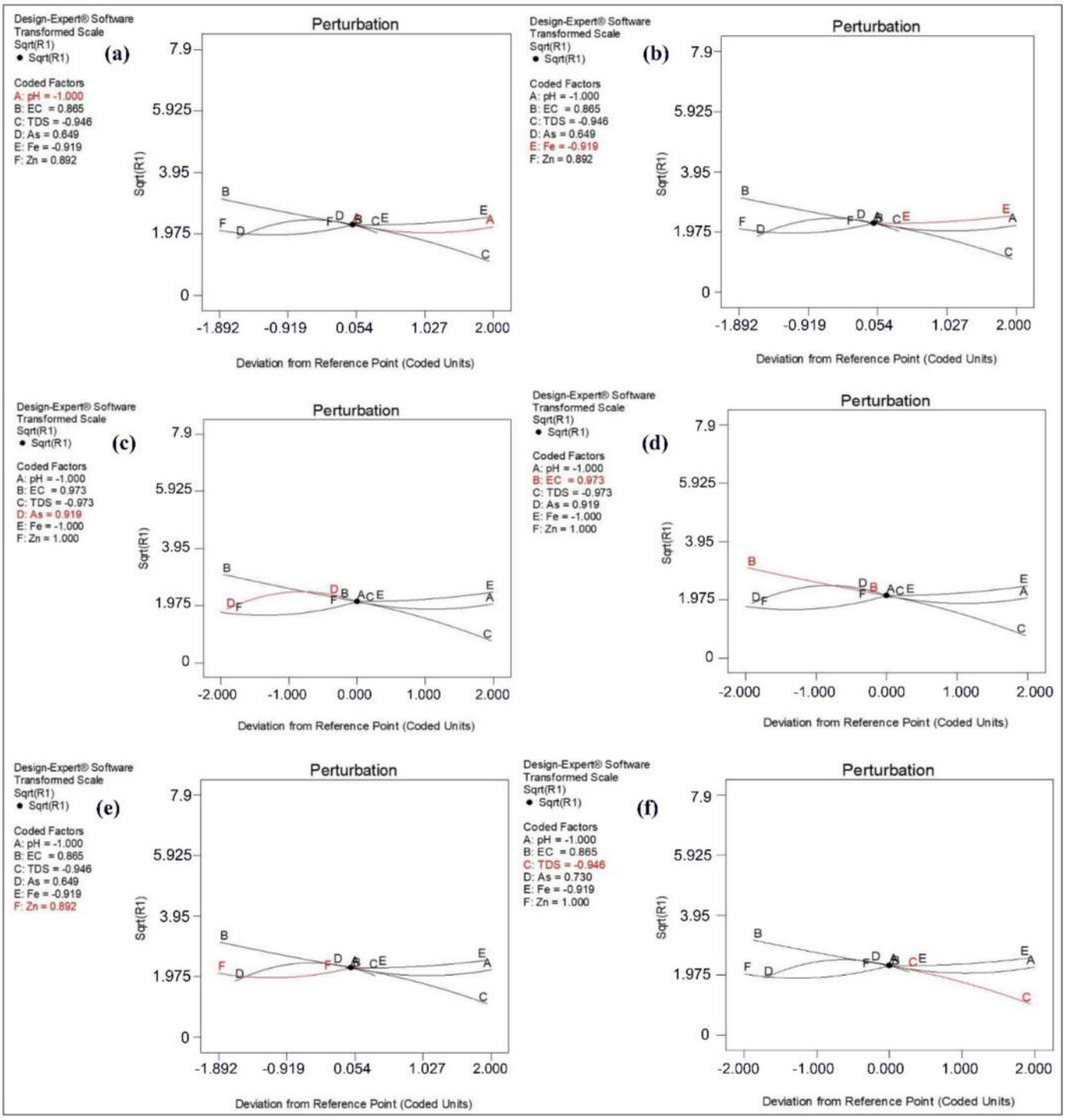

Fig. 7. Coding effects at the main deviation reference point, based on coded values of groundwater constituents, including heavy metals.

Individual HQ values for As, Fe, and Zn were below 1 for both adults and children in most cases, suggesting limited non-carcinogenic risk from any single metal when considered alone (Bodrud-Doza et al., 2019; Zhang et al., 2016). Fig. 9 (a–h) and Table 1 summarize the spatial distribution of HQ/HI and CR for adults and children across aquifers in the coastal study area, consistent with USEPA (2009) risk characterization.

Oral exposure:

- Adults: Oral HI for As, Fe, and Zn ranged from 0.00032 to 3.262. Approximately 45 % of adult samples fall into the high-risk HI category (Fig. 9a; Table 1).
- Children: Oral HI ranged from 0.0002 to 1.237 (median 0.008). About 35 % of children show high oral HI (Fig. 9h; Table 1).
- Carcinogenic risk (CR): Adult oral CR ranges from 0.00078 to 0.756, while children range from 0.00045 to 0.0076 (median 0.0011). Approximately 25 % of adults exhibit high oral CR (Fig. 9g), and 25 % of children show high oral CR (Fig. 9b; Table 1).

Dermal exposure:

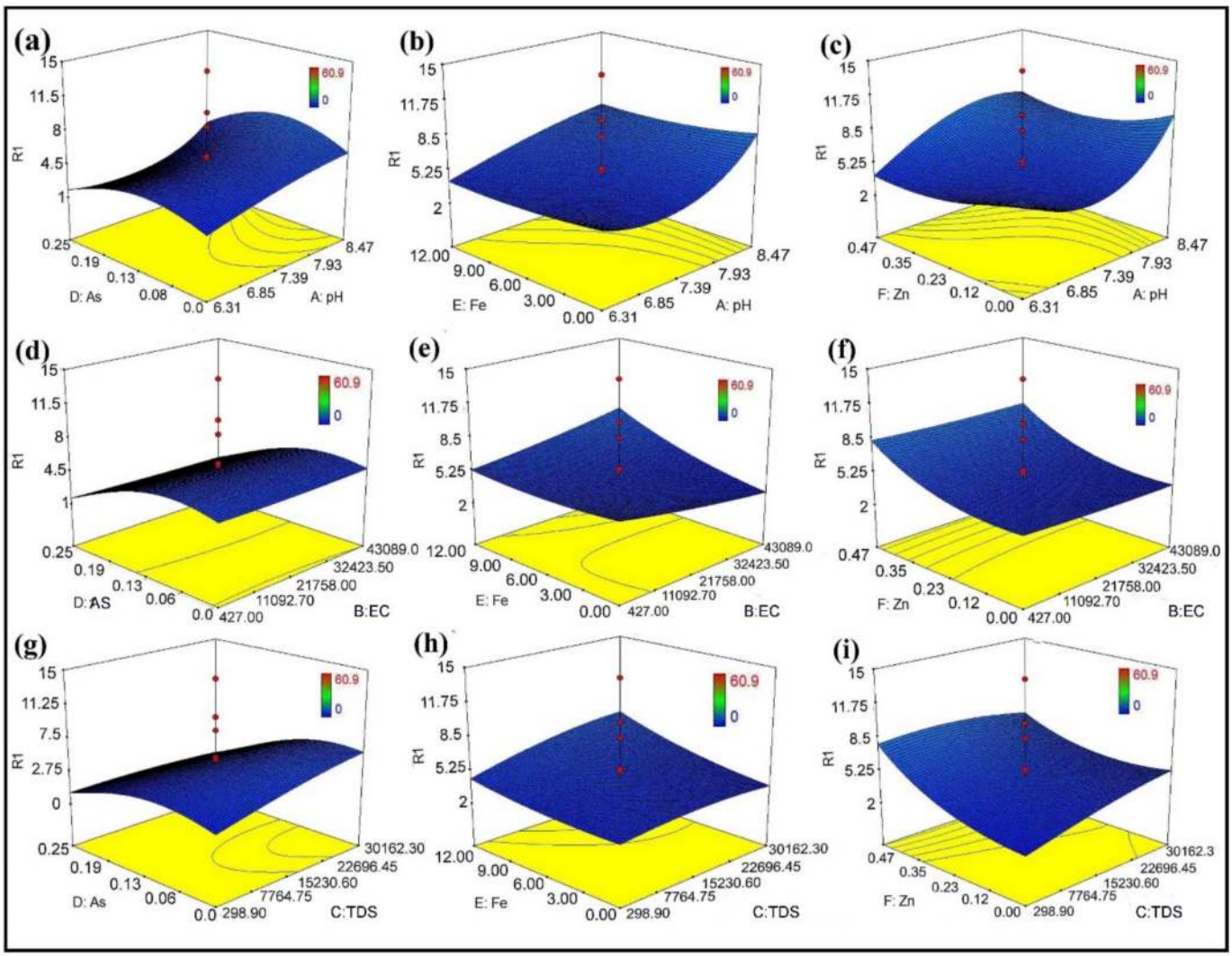

Fig. 8. Three-dimensional diagrams illustrating the combined effects of hydrochemistry and heavy metals on the outcome metric; the NPI is highlighted at R1.

- Adults: Dermal HI ranges from 0 to 4.562 (median 0.021). Roughly 40 % of adult dermal samples are in the high-risk CR category (Fig. 9d).
- Children: Dermal HI ranges from 0.0008 to 3.500 (median 0.234). Approximately 65 % of children/adolescents are classified as high risk by dermal HI (Fig. 9c), and about 45 % show high dermal CR (Fig. 9f; Table 1).
- Dermal CR: Adults range from 0.00058 to 0.008; children range from 0.00076 to 0.067 (mean 0.0096; mode 0.00036).

Overall, As remains the dominant driver of risk, with geospatial clustering of higher HI and CR consistent with prior work in coastal and industrial settings (Hasan et al., 2020; Karim, 2011; Siegel, 2002). While dermal risks are often reported to be lower than ingestion risks (Gao et al., 2021), the high-risk fractions observed here—particularly for children—underscore the need for targeted risk management. Similar evaluations elsewhere show variability due to hydrogeology, source inputs, and water-use behavior (Gao et al., 2021; Wang et al., 2021; Zhang et al., 2016). Taken together, accumulated oral and dermal exposures may pose non-carcinogenic and carcinogenic risks to local populations, and some CR values appear to exceed commonly referenced acceptable ranges, warranting precautionary action.

4.8. Recommendations, prospects, and constraints

4.8.1. Suggestions for sustainable management

Based on these results, we acknowledge that preventing and managing saltwater intrusion is crucial for preserving groundwater quality and minimizing the buildup of toxic heavy metals like As, Zn, and Fe. Here are some key recommendations to tackle this pressing issue:

1. **Strengthen Oversight of Groundwater Extraction**: Coastal governments and companies should enhance their oversight of groundwater extraction and implement strict regulations on freshwater use. Key actions include:

- Increasing the number of groundwater monitoring stations.
- Improving detection technologies for early identification of saltwater intrusion.
- Reducing excessive groundwater extraction.

For example, in Longkou, located on the eastern coast of Laizhou Bay, China, a comprehensive system of wells has been established since 1989 to monitor saltwater incursion effectively (Xue et al., 1993).

2. **Implement Water-Saving Technologies**: Continuous upgrades to detection infrastructure for seawater intrusion have led to the

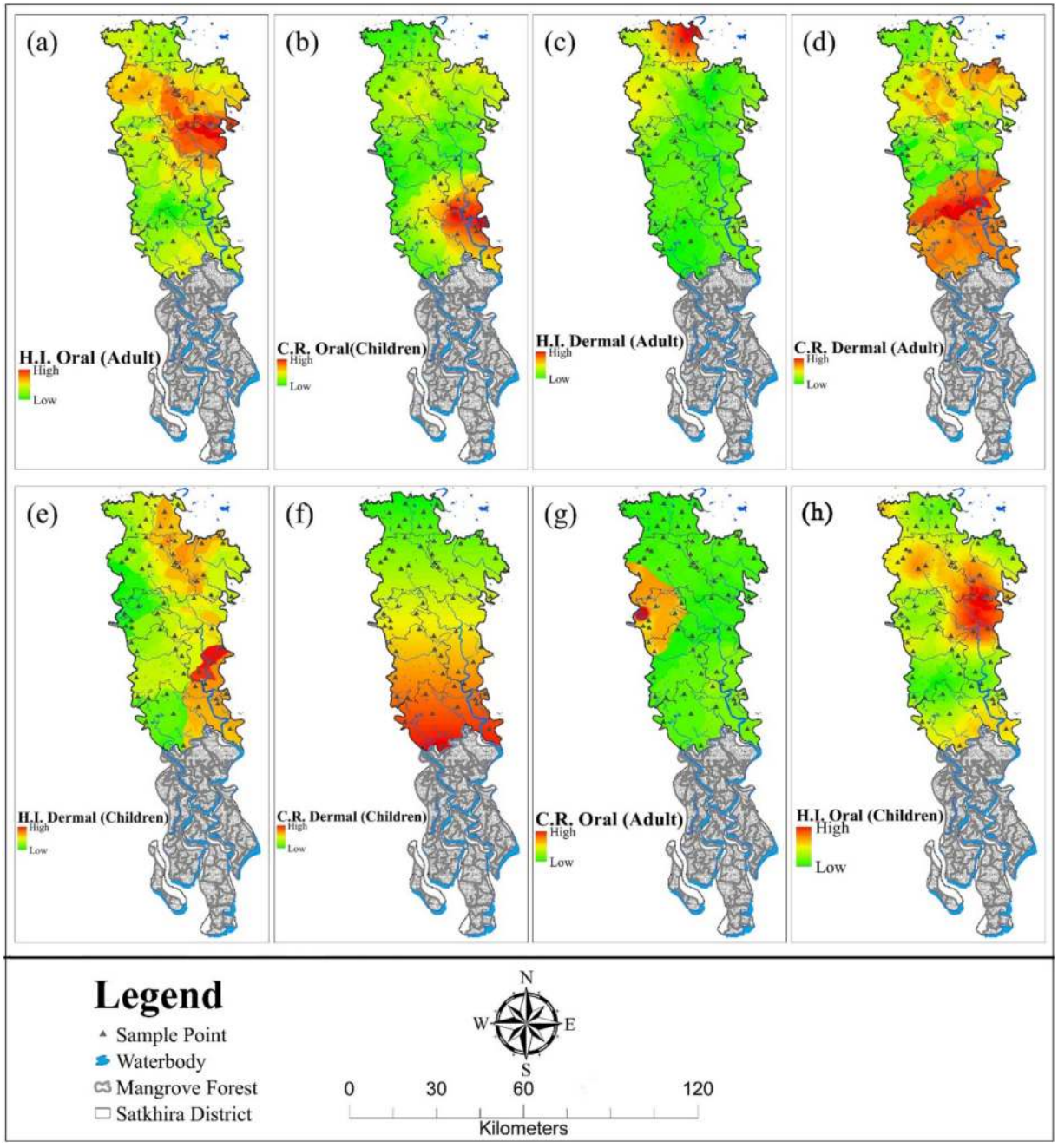

Fig. 9. The spatial distribution of HI and CR is spread across the categories of adult and children for oral and dermal exposure.

development of a comprehensive monitoring system. Previous studies (Ke et al., 2021; Shi and Jiao, 2014; Wang et al., 2021) show that water-saving technologies can significantly:

- Reduce agricultural water usage.
- Enhance groundwater availability, thereby helping to mitigate saltwater intrusion.

3. **Purify and Distribute Freshwater**: In regions affected by saltwater intrusion, it is vital to centrally purify freshwater and distribute it to local communities (Chiamsathit et al., 2020; Zhang et al., 2016). This initiative not only helps to reduce health risks associated with contaminated groundwater but also addresses issues related to unregulated extraction. Actions may be executed in the following ways:

- Always use safe water that has been treated, bottled, or tested at a recognised facility for drinking, preparing, and cooking. Likewise, the inhabitants can store rainwater and use it for their daily needs as an alternative safe source.
- The government needs to promote regular inspections of wells and point-of-use treatments, offering them free of charge (such as authorised As and Fe removal filters).

4. **Address Industrial Contributions to Contamination**: Industrial activities can contribute to the contamination of freshwater sources with heavy metals (Chiamsathit et al., 2020; Datta et al., 2020; Xue et al., 1993). To combat this, it is essential to:

- Enhance oversight of industrial wastewater discharges.

Table 1
Population- and pathway-specific risk levels (%) derived from spatial analysis (oral and dermal; adults and children).

Fig. reference.	Exposure pathway & inhabitants categories	Risk level (%)
Fig. 9a	Oral – Adults	High: 45 % Low: 25 % No Risk: 30 %
Fig. 9b	Oral – Children	High: 25 % Low: 15 % No Risk: 55 %
Fig. 9c	H.I. - Dermal – Adolescents	High: 65 % Relatively Safe: 20 % No Risk: 15 %
Fig. 9d	C.R.- Dermal – Adults	High: 40 % Low: 5 % No Risk: 45 %
Fig. 9e	H.I.- Dermal – Children	High: 45 % Moderate: 35 % No Risk: 20 %
Fig. 9f	C.R.- Dermal Risk – Children	High: 35 % Moderate: 25 % No Risk: 40 %
Fig. 9g	C.R. – Oral Adults	High: 25 % Moderate: 10 % No Risk: 65 %
Fig. 9h	H.I.- Oral– Children	High: 35 % Moderate: 25 % No Risk: 40 %

- Promote awareness and adoption of cleaner manufacturing technologies.

4.8.2. *Limitations and future prospects*

This study analyzed heavy metal contamination in groundwater and associated health hazards. However, the source analysis focused on three major heavy metals and their ions, omitting other potentially harmful metals. To enhance the accuracy of future findings, comprehensive surveys incorporating data on body weight, consumption rates, and exposure duration among the local population are recommended. Further research should also include a broader range of heavy metals and pollutants for a more comprehensive understanding of groundwater contamination. This could include analyzing seasonal variations in metal levels and health risks over time to inform the development of new or adjusted regulations for local industries.

Future research should explore cost-effective methods for removing heavy metals and other hazards from groundwater before consumption. Correlating well samples near rivers, industrial sites, coastal areas, and populated areas with specific sampling conditions is crucial for reducing health risks. Seasonal assessments of metal concentrations are also needed to better understand their impact on public health.

5. Conclusion

This study investigated the chemical properties of groundwater, the distribution of heavy metals, and associated health risks in Bangladesh's Satkhira District, focusing on the impact of rapid industrial growth in coastal areas. Key findings include:

- Source Identification: Correlation matrix and PCA analyses revealed significant correlations between Zn, Fe, and As with alkaline dominant components (Na and Cl) in coastal regions, indicating both natural and anthropogenic sources. Furthermore, RSM-ANOVA demonstrated optimal correlations for heavy metal indices with major components through 3D coded analysis.
- Aquifer Characterization: An alkaline-clay-dominated aquifer was identified, characterized by a dominant 'NaCl-type' and a less dominant 'HCO_3-type' water. Significant cation and anion proportions were: $Na^+ > Mg^{2+} > Ca^{2+} > K^+$ and $Cl^- > HCO_3^- > SO_4^{2-} > CO_3^{2-}$, respectively.
- Pollution Levels: Heavy metal indices (HMEI, HMI, NPI, and C_d) revealed that significant heavy metal pollution highly affects 30 %, 68 %, 39 %, and 19 % of the areas, respectively.
- The HRA indicated significant CR and HI for both adults and children, mainly due to elevated Fe and Zn, and moderate As levels. Sites with the highest HQ for oral and dermal exposure to As, Fe, and Zn showed a higher percentage of reduced contamination risk for both adults and children. In most test sites, HQ values exceeded one for the sequence Fe > Zn > As, raising concerns about acute and long-term health hazards.
- Environmental Injustice and Policy Implications: Geospatial visualizations highlight the severe environmental injustice and metal pollution affecting local populations, extending beyond residents. These findings provide a framework for future policy recommendations and research. The southern coastal region shows heavy metal pollution, increasing chronic health risks. Residents should avoid using local aquifers for drinking water and seek alternative sources.

CRediT authorship contribution statement

Md Yeasir Hasan: Methodology, Investigation, Formal analysis, Data curation, Conceptualization, Writing – original draft. **Xiaolang Zhang:** Supervision, Formal analysis, Data curation, Conceptualization, Writing – review & editing. **Chao Xu:** Supervision, Formal analysis, Conceptualization, Writing – review & editing. **Jay Sui Tung:** Supervision, Writing – review & editing. **Abir Ahmed Rifat:** Methodology, Investigation, Formal analysis, Data curation. **M. Shahriar Sonet:** Formal analysis, Data curation. **Abdulla-Al Kafy:** Software, Formal analysis. **Shaikh Sadiqur Rahman:** Formal analysis. **Md Jamal Faruque:** Supervision, Formal analysis, Data curation.

Declaration of generative AI and AI-assisted technologies in the writing process

During the preparation of this work the authors used Ernie Bot and AskGPT in order to improve the readability and language of the manuscript. After using these tools/services, the authors reviewed and edited the content as needed and take full responsibility for the content of the published article.

Declaration of competing interest

The authors declare that they have no known competing financial interests or personal relationships that could have appeared to influence the work reported in this paper.

Appendix A. Supplementary data

Supplementary data to this article can be found online at https://doi.org/10.1016/j.scitotenv.2025.180640.

Data availability

Data will be made available on request.

References

Ahmed, M.T., Firoz, M.G., Islam, M.S., Hasan, M.Y., 2019a. Extraction of Aluminium Sulphate and copper Sulphate from printed circuit board as E-waste. Int. Adv. Res. J. Sci. Eng. Technol. (IARJSET) 6 (11), 1–5. https://doi.org/10.17148/IARJSET.2019.61101.

Ahmed, M.T., Hasan, M.Y., Khan, A.S., Hasan, M., 2019b. Valuation of irrigation water at Shagordari, Jashore, Bangladesh. Int. Res. J. Eng. Technol. (IRJET) 06 (11), 1050–1057.

Ahmed, M.T., et al., 2020a. Monitoring of groundwater quality in arsenic and salinity prone areas of Jashore. Bangladesh. Int. J. Econ. Environ. Geol. 11 (1), 83–88. https://doi.org/10.46660/ijeeg.Vol11.Iss1.2020.417.

Ahmed, M.T., et al., 2020b. Hydro-geochemical evaluation of groundwater with studies on water quality index and suitability for drinking in Sagardari. Jashore. J. Groundw. Sci. Eng. 8 (3), 259–273. https://doi.org/10.19637/j.cnki.2305-7068.2020.03.006.

Ahmed, M.T., et al., 2021a. Evaluation of groundwater quality and its suitability by applying the geospatial and IWQI techniques for irrigation purposes in the southwestern coastal plain of Bangladesh. Arab. J. Geosci. 14, 1–24. https://doi.org/10.1007/s12517-021-06510-y.

Ahmed, M.T., et al., 2021b. Evaluation of groundwater quality and its suitability by applying the geospatial and IWQI techniques for irrigation purposes in the southwestern coastal plain of Bangladesh. Arab. J. Geosci. 14 (3), 1–24. https://doi.org/10.1007/s12517-021-06510-y.

Ahmed, M.T., et al., 2022. Hydrochemical investigations of coastal aquifers and saltwater intrusion in severely affected areas of Satkhira and Bagerhat districts. Bangladesh. Arab. J. Geosci. 15 (8), 1–22. https://doi.org/10.1007/s12517-022-09955-x.

Ahmed, N., et al., 2019c. Hydrogeochemical evaluation and statistical analysis of groundwater of Sylhet, North-Eastern Bangladesh. Acta Geochim. 38 (3), 440–455. https://doi.org/10.1007/s11631-018-0303-6.

Ani, I., Okafor, J., Olutoye, M., Akpan, U., 2015. Optimization of base oil regeneration from spent engine oil via solvent extraction. Adv. Dent. Res. 4 (6), 403–411. https://doi.org/10.9734/AIR/2015/16795.

APHA, A.P.H.A., 2023. Standard Methods for the Examination of Water and Wastewater. American public health association.,. APHA Press, Washington, DC. https://doi.org/10.2105/SMWW.2882.

Backman, C., Mackie, H., 1997. Reliability and validity of the arthritis hand function test in adults with osteoarthritis. Occup. Ther. J. Res. 17 (1), 55–66. https://doi.org/10.1177/153944929701700104.

Barakat, M., 2011. New trends in removing heavy metals from industrial wastewater. Arab. J. Chem. 4 (4), 361–377. https://doi.org/10.1016/j.arabjc.2010.07.019.

Bayuo, J., Abukari, M.A., Pelig-Ba, K.B., 2019. Equilibrium isotherm studies for the sorption of hexavalent chromium (VI) onto groundnut shell. IOSR J Appl Chem (IOSR-JAC) 11 (12), 40–46. https://doi.org/10.9790/5736-11120 14046.

Bhuiyan, M.A.H., et al., 2016. Assessment of groundwater quality of Lakshimpur district of Bangladesh using water quality indices, geostatistical methods, and multivariate analysis. Environ. Earth Sci. 75 (12), 1–23. https://doi.org/10.1007/s12665-016-5823-y.

Bodrud-Doza, M., et al., 2019. Groundwater pollution by trace metals and human health risk assessment in central west part of Bangladesh. Groundw. Sustain. Dev. 9, 100219. https://doi.org/10.1016/j.gsd.2019.100219.

Chakraborty, S., et al., 2014. Experimental analysis, modeling and optimization of chromium (VI) removal from aqueous solutions by polymer-enhanced ultrafiltration. J. Membr. Sci. 456, 139–154. https://doi.org/10.1016/j.memsci.2014.01.016.

Chiamsathit, C., Auttamana, S., Thammarakcharoen, S.J.A.W.S., 2020. Heavy metal pollution index for assessment of seasonal groundwater supply quality in hillside area, Kalasin. Thailand. Appl. Water Sci. 10 (6), 1–8. https://doi.org/10.1007/s13201-020-01230-2.

Datta, D.K., Ghosh, P.K., Karim, M.R., Rahman, M.M., 2020. Geochemical options for water security in a coastal urban agglomerate of lower Bengal Delta. Bangladesh. J. Geochem. Explor. 209, 106440. https://doi.org/10.1016/j.gexplo.2019.106440.

Dola, S.S., Bahsar, K., Islam, M., Sarker, M.M.R., 2018. Hydrogeological classification and the correlation of groundwater chemistry with basin flow in the south-western part of Bangladesh. J. Bangla. Acad. Sci. 42 (1), 41–54. https://doi.org/10.3329/jbas.v42i1.37831.

Durov, S., 1948. Natural waters and graphic representation of their composition. Dokl. Akad. Nauk SSSR 87–90.

Edet, A., Offiong, O., 2002. Evaluation of water quality pollution indices for heavy metal contamination monitoring. A study case from Akpabuyo-Odukpani area, lower Cross River basin (southeastern Nigeria). GeoJournal 57 (4), 295–304. https://doi.org/10.1023/B:GEJO.0000007250.92458.de.

Faruque, M.J., et al., 2022. Monitoring of land use and land cover changes by using remote sensing and GIS techniques at human-induced mangrove forests areas in Bangladesh. Remote Sens. Appl. Soc. Environ. 25, 100699. https://doi.org/10.1016/j.rsase.2022.100699.

Gao, Z., et al., 2021. Assessment of the water quality of groundwater in Bohai rim and the controlling factors—a case study of northern Shandong peninsula, North China. Environ. Pollut. 285, 117482. https://doi.org/10.1016/j.envpol.2021.117482.

Garba, Z.N., Bello, I., Galadima, A., Lawal, A.Y., 2016. Optimization of adsorption conditions using central composite design for the removal of copper (II) and lead (II) by defatted papaya seed. Karbala Int. J. Mod. Sci. 2 (1), 20–28. https://doi.org/10.1016/j.kijoms.2015.12.002.

Hasan, M.Y., et al., 2020. Dataset on the evaluation of hydrochemical properties and groundwater suitability for irrigation purposes: south-western part of Jashore. Bangladesh. Data in Brief 32, 106315. https://doi.org/10.1016/j.dib.2020.106315.

ISO, 2009. 5667–11: 2009—Water Quality—Sampling—Part 11: Guidance on Sampling of Groundwaters. Geneva, Switzerland, International Organization for Standarization.

ISO, 2023. Water quality — Sampling- Part 1: Guidance on the design of sampling programmes and sampling techniques, 39 pp.

Jahin, H.S., Abuzaid, A.S., Abdellatif, A.D., 2020. Using multivariate analysis to develop irrigation water quality index for surface water in Kafr El-Sheikh governorate. Egypt. Environ. Technol. Innov. 17, 100532. https://doi.org/10.1016/j.eti.2019.100532.

Kanagaraj, G., Elango, L., Sridhar, S., Gowrisankar, G., 2018. Hydrogeochemical processes and influence of seawater intrusion in coastal aquifers south of Chennai, Tamil Nadu. India. Environ. Sci. Polluti. Res. 25 (9), 8989–9011. https://doi.org/10.1007/s11356-017-0910-5.

Karim, Z., 2011. Risk assessment of dissolved trace metals in drinking water of Karachi, Pakistan. Bull. Environ. Contam. Toxicol. 86, 676–678. https://doi.org/10.1007/s00128-011-0261-8.

Kavitha, E., et al., 2019. Removal and recovery of heavy metals through size enhanced ultrafiltration using chitosan derivatives and optimization with response surface modeling. Int. J. Biol. Macromol. 132, 278–288. https://doi.org/10.1016/j.ijbiomac.2019.03.128.

Ke, S., Chen, J., Zheng, X., 2021. Influence of the subsurface physical barrier on nitrate contamination and seawater intrusion in an unconfined aquifer. Environ. Pollut. 284, 117528. https://doi.org/10.1016/j.envpol.2021.117528.

Kibria, G., Hossain, M.M., Mallick, D., Lau, T.C., Wu, R., 2016. Trace/heavy metal pollution monitoring in estuary and coastal area of bay of Bengal, Bangladesh and implicated impacts. Mar. Pollut. Bull. 105 (1), 393–402. https://doi.org/10.1016/j.marpolbul.2016.02.021.

Liu, Z., Liu, C., Mostafavi, A., 2023. Beyond residence: a mobility-based approach for improved evaluation of human exposure to environmental hazards. Environ. Sci. Technol. 57 (41), 15511–15522. https://doi.org/10.1021/acs.est.3c04691.

Mahapatra, S., Venugopal, T., Shanmugasundaram, A., Giridharan, L., Jayaprakash, M., 2020. Heavy metal index and geographical information system (GIS) approach to study heavy metal contamination: a case study of North Chennai groundwater. Appl Water Sci 10 (12), 1–17. https://doi.org/10.1007/s13201-020-01321-0.

Monir, M.U., et al., 2021. Optimization of fuel properties in two different peat reserve areas using surface response methodology and square regression analysis. Biomass Convers. Biorefinery 1-21. https://doi.org/10.1007/s13399-021-01656-x.

Najafpour, A., Khorrami, A.R., Azar, P.A., Tehrani, M.S., 2020. Study of heavy metals biosorption by tea fungus in Kombucha drink using central composite design. J. Food Compos. Anal. 86, 103359. https://doi.org/10.1016/j.jfca.2019.103359.

Nkpaa, K., Amadi, B., Wegwu, M.J.H., Journal, E.R.A.A.I., 2018. Hazardous metals levels in groundwater from Gokana, Rivers state, Nigeria: non-cancer and cancer health risk assessment. Hum. Ecol. Risk Assess. Int. J. 24 (1), 214–224. https://doi.org/10.1080/10807039.2017.1374166.

Pearson, K., 1901. LIII. On lines and planes of closest fit to systems of points in space. The London, Edinburgh, and Dublin Philos. Mag. J. Sci. 2 (11), 559–572. https://doi.org/10.1080/14786440109462720.

Piper, A.M., 1944. A graphic procedure in the geochemical interpretation of water-analyses. EOS Trans. Am. Geophys. Union 25 (6), 914–928. https://doi.org/10.1029/TR025i006p00914.

Rahman, M.A.T., et al., 2020. Heavy metal pollution assessment in the groundwater of the Meghna Ghat industrial area, Bangladesh, by using water pollution indices approach. Appl Water Sci 10 (8), 1–15. https://doi.org/10.1007/s13201-020-01266-4.

Rahman, M.M., et al., 2023. Drinking water quality assessment based on index values incorporating WHO guidelines and Bangladesh standards. Phys. Chem. Earth, Parts A/B/C 129, 103353. https://doi.org/10.1016/j.pce.2022.103353.

Rahman, M.T.U., et al., 2016. Mobilization of high arsenic in the shallow groundwater of Kalaroa, South-Western Bangladesh. Expo. Health 8, 159–175. https://doi.org/10.1007/s12403-015-0177-3.

Rakib, M.R.J., et al., 2022. A comprehensive review of heavy metal pollution in the coastal areas of Bangladesh: abundance, bioaccumulation, health implications, and challenges. Environ. Sci. Pollut. Res. 29 (45), 67532–67558. https://doi.org/10.1007/s11356-022-22122-9.

Saha, R., Dey, N.C., Rahman, M., Bhattacharya, P., Rabbani, G.H., 2019. Geogenic arsenic and microbial contamination in drinking water sources: exposure risks to the coastal population in Bangladesh. Front. Environ. Sci. 7, 57. https://doi.org/10.3389/fenvs.2019.00057.

Sarker, M.M.R., et al., 2022a. Identifying the major hydrogeochemical factors governing groundwater chemistry in the coastal aquifers of Southwest Bangladesh using statistical analysis. Hydrology 9 (2), 20. https://doi.org/10.3390/hydrology9020020.

Sarker, M.M.R., et al., 2022b. Hydrochemical characterization and groundwater potential of the deep aquifer system in southwest coastal region of Bangladesh. J. Asian Earth Sci. 234, 105271. https://doi.org/10.1016/j.jseaes.2022.105271.

Sharmin, S., Mia, J., Miah, M.S., Zakir, H., 2020. Hydrogeochemistry and heavy metal contamination in groundwaters of Dhaka metropolitan city, Bangladesh: assessment of human health impact. HydroResearch 3, 106–117. https://doi.org/10.1016/j.hydres.2020.10.003.

Shi, L., Jiao, J.J., 2014. Seawater intrusion and coastal aquifer management in China: a review. Environ. Earth Sci. 72, 2811–2819. https://doi.org/10.1007/s12665-014-3186-9.

Siegel, F.R., 2002. Environmental geochemistry of potentially toxic metals, 32. Springer. https://doi.org/10.1007/978-3-662-04739-2.

Singh, A.K., Sathya, M., Verma, S., Jayakumar, S., 2018. Health risk assessment of heavy metals in crop grains grown on open soils of Kanwar wetland, India. Euro-Mediterr. J. Environ. Integr. 3 (1), 29. https://doi.org/10.1007/s41207-018-0073-x.

Sonet, M.S., Hasan, M.Y., Kafy, A.A., Shobnom, N., 2025. Spatiotemporal analysis of urban expansion, land use dynamics, and thermal characteristics in a rapidly growing megacity using remote sensing and machine learning techniques. Theor. Appl. Climatol. 156 (2), 79. https://doi.org/10.1007/s00704-024-05264-3.

Standard, B.J.G.o.t.P.s.R.o.B., Dhaka, 1997. The environment conservation rules 1997.

Tasnim, F., et al., 2025. An assessment of the spatial and temporal distribution of nitrate and trace element concentrations in groundwater in coastal districts of Bangladesh. Sci. Total Environ. 970, 178988. https://doi.org/10.1016/j.scitotenv.2025.178988.

USEPA, 2004. Risk assessment guidance for superfund.

USEPA, 2009. National Primary and Secondary Drinking Water Standards.

Vetrimurugan, E., Brindha, K., Elango, L., Ndwandwe, O.M., 2017. Human exposure risk to heavy metals through groundwater used for drinking in an intensively irrigated river delta. Appl Water Sci 7, 3267–3280. https://doi.org/10.1007/s13201-016-0472-6.

Wang, Z., Su, Q., Wang, S., Gao, Z., Liu, J., 2021. Spatial distribution and health risk assessment of dissolved heavy metals in groundwater of eastern China coastal zone. Environ. Pollut. 290, 118016. https://doi.org/10.1016/j.envpol.2021.118016.

Wu, J., et al., 1993. Sea-water intrusion in the coastal area of Laizhou Bay, China: 2. Sea-water intrusion monitoring. Groundwater 31 (5), 740–745. https://doi.org/10.1111/j.1745-6584.1993.tb00845.x.

Xue, Y., et al., 1993. Sea-water intrusion in the coastal area of Laizhou Bay, China: 1. Distribution of sea-water intrusion and its hydrochemical characteristics. Groundwater 31 (4), 532–537. https://doi.org/10.1111/j.1745-6584.1993.tb00584.x.

Yu, C.H., et al., 2025. Biomonitoring of toxic metal exposure in New Jersey adults in 2015–2018. Int. J. Hyg. Environ. Health 264, 114510. https://doi.org/10.1016/j.ijheh.2024.114510.

Zakir, H., Sharmin, S., Akter, A., Rahman, M.S., 2020. Assessment of health risk of heavy metals and water quality indices for irrigation and drinking suitability of waters: a case study of Jamalpur Sadar area. Bangladesh. Environ. Adv. 2, 100005. https://doi.org/10.1016/j.envadv.2020.100005.

Zhang, S., Liu, G., Sun, R., Wu, D., 2016. Health risk assessment of heavy metals in groundwater of coal mining area: a case study in Dingji coal mine, Huainan coalfield, China. Hum. Ecol. Risk Assess. Int. J. 22 (7), 1469–1479. https://doi.org/10.1080/10807039.2016.1185689.